The numerical wind atlas - the KAMM/WAsP method

Frank, H.P.; Rathmann, Ole; Mortensen, Niels Gylling; Landberg, L.

Publication date:
2001

Document Version
Publisher's PDF, also known as Version of record

Risø–R–1252(EN)

The Numerical Wind Atlas

—

the KAMM/WA^{S}P Method

Helmut P. Frank, Ole Rathmann, Niels G. Mortensen, Lars Landberg

Risø National Laboratory, Roskilde, Denmark
June 2001

Abstract The method of combining the Karlsruhe Atmospheric Mesoscale Model, KAMM, with the Wind Atlas Analysis and Application Program, WAsP, to make local predictions of the wind resource is presented. It combines the advantages of meso-scale modeling — overview over a big region and use of global data bases — with the local prediction capacity of the small-scale model WAsP. Results are presented for Denmark, Ireland, Northern Portugal and Galicia, and the Faroe Islands.

Wind atlas files were calculated from wind data simulated with the meso-scale model using model grids with a resolution of 2.5, 5, and 10 km. Using these wind atlas files in WAsP the local prediction of the mean wind does not depend on the grid resolution of the meso-scale model. The local predictions combining KAMM and WAsP are much better than simple interpolation of the wind simulated by KAMM.

In addition an investigation was made on the dependence of wind atlas data on the size of WAsP-maps. It is recommended that a topographic map around a site should extend 10 km out from it. If there is a major roughness change like a coast line further away in a frequent wind direction this should be included at even greater distances, perhaps up to 20 km away.

ISBN 87–550–2850–0; ISBN 87-550-2909-4 (internet)
ISSN 0106–2840

Print: Danka Services International · 2001

Contents

1 Introduction

The Wind Atlas Analysis and Application Program WAsP (Mortensen et al., 1998, 1993) is a tested tool to make predictions of the wind energy potential from high quality wind measurements. It estimates the local influences on the wind by small hills, roughness changes, (see e.g., Mortensen and Petersen, 1998) and obstacles like trees or buildings to generate a wind atlas of "cleaned" measurements. This wind atlas is used to make predictions at other sites with a similar wind climate (see e.g., Troen and Petersen, 1989).

Unfortunately, in many parts of the world there is only poor or no wind data available. On the other hand, global weather models make analyses also in these areas, e.g. the re-analysis projects at NCEP/NCAR (Kalnay et al., 1996), ECMWF (Gibson et al., 1997), or NASA (Schubert et al., 1993). These analyses are too coarse to be used directly for wind power applications. However, they can provide boundary conditions and external forcing for atmospheric meso-scale models.

Meso-scale models make wind prediction for larger regions of several ten thousand square kilometers. To cover a similar area with measurements would require many stations. This is costly, and it takes a long time to obtain climatological estimates. Therefore, meso-scale models promise to be good tools to obtain an overview of the wind resource of an entire region. However, they can not be used for the siting of wind turbines because the grid resolution of these models is too big.

This project investigated a way of combining both types of models employing the wind atlas concept as used in WAsP. The Karlsruhe Atmospheric Mesoscale Model KAMM (Adrian and Fiedler, 1991; Adrian, 1994) is used to simulate the wind field for a region. It is forced by data from the global NCEP/NCAR reanalysis (Kalnay et al., 1996). The simulated wind fields are processed into wind atlas files which can be read by WAsP to make local predictions of the wind resource. The combination of KAMM and WAsP was first used by Landberg and Watson (1994). Further calculations for Ireland are presented in Frank and Landberg (1996, 1997, 1998).

The concept is described in the next section. The main part presents the analysis for different regions: Denmark, Ireland, northern Portugal and Galicia, and the Faroe Islands. The discussion of data and errors is summarized before the regions in sections 3 and 5. Section 4 is a bit separate from the rest to investigate the effects the size of the topographic maps for WAsP on wind atlas data generated by WAsP. The conclusions are presented in the last section.

2 Basic Ideas and Models

2.1 The wind atlas method

The wind atlas methodology in its present form was developed for the analysis presented in the European Wind Atlas (Troen and Petersen, 1989). The methodology employs a comprehensive set of models for the horizontal and vertical extrapolation of wind data and the estimation of wind climate and wind resources. The actual implementation of the models is known as the *Wind Atlas Analysis and Application Program* (WAsP) which is the software package (Mortensen et al., 1993, 1998) that has been applied for the present study.

The WAsP models are based on the physical principles of flows in the atmospheric

boundary layer and they take into account the effects of different surface roughness conditions, sheltering effects due to buildings and other obstacles, and the modification of the wind imposed by the specific terrain height variations around the meteorological station in question. Figure 1 illustrates the use of these models on measured wind data to calculate a regional wind climatology or wind atlas.

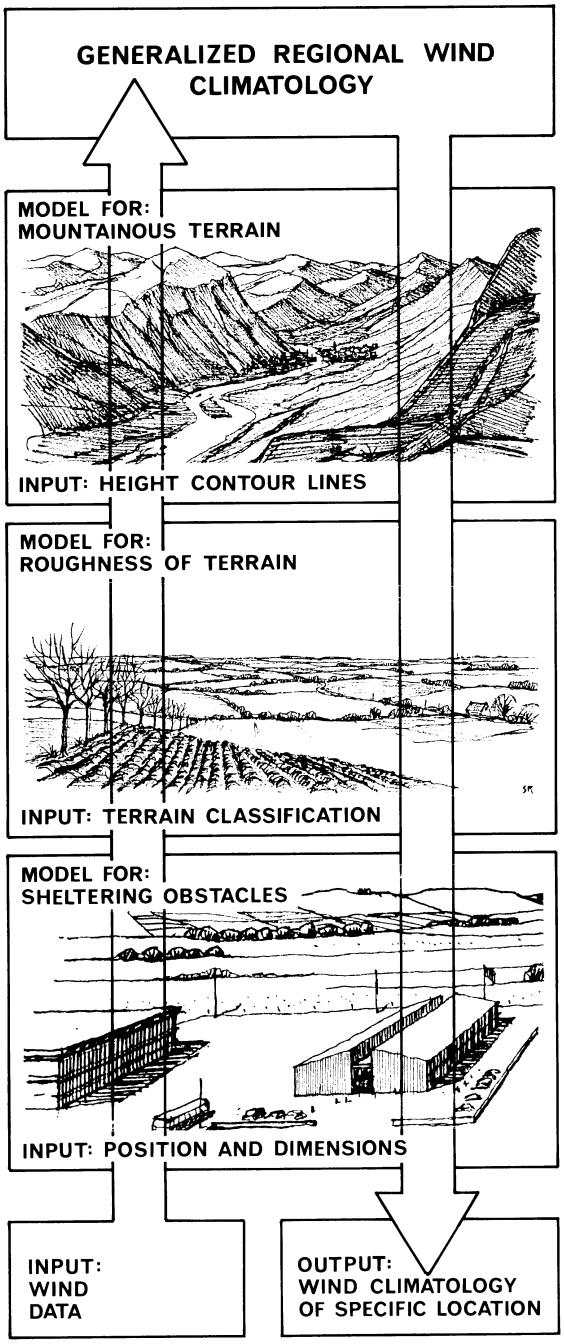

Figure 1. The wind atlas methodology of WASP. Meteorological models are used to calculate the regional wind climatologies from the raw data. In the reverse process – the application of wind atlas data – the wind climate at any specific site may be calculated from the regional climatology.

The figure also illustrates the so-called application part of the methodology, following a procedure in which the regional wind climatology is used as input to the same models to produce a site-specific wind climatology and, given the power curve of a wind turbine, a production estimate. The *analysis* and *application* parts of the program can thus be summarized in the following way:

Analysis:

time-series of wind speed and direction $\rightarrow$ wind statistics

wind statistics + met. site description $\rightarrow$ wind atlas data

Application:

wind atlas data + site description $\rightarrow$ est. wind climate

estimated wind climate + power curve $\rightarrow$ est. power production

The WASP program enables an analysis of any time-series of wind speed and direction measurements. The output is a wind rose and the wind speed distributions in the different sectors. A Weibull distribution function is then fitted to the measured histograms to provide scale and shape parameters A and k for each sector.

The observed wind data are converted into a wind atlas data set by invoking the shelter, roughness and flow models in WASP; using descriptions of the topography of the meteorological station as input. In a wind atlas data set the wind distributions have been "cleaned" with respect to the site-specific conditions and reduced to standard conditions, e.g. transformed into Weibull A- and k-parameters for 4 standard roughnesses, 5 standard heights above ground and 12 azimuth sectors.

Using a wind atlas data set calculated as described above or one obtained from another source – e.g. the European Wind Atlas – the program can estimate the wind climate at any particular point by performing the inverse calculation as is used to generate a wind atlas, i.e. by reintroducing the actual topographic conditions of the application or predicted site. Furthermore, the total energy content of the mean wind can be calculated from the predicted wind speed distributions and an estimate of the actual, yearly mean power production of a wind turbine can be obtained; given the power curve of the turbine in question.

Accurate predictions using the WASP program may be obtained (Bowen and Mortensen, 1996; Mortensen and Petersen, 1998) provided: i) the reference site (meteorological station) and predicted site are subject to the same overall weather regime, ii) the prevailing weather conditions are close to being neutrally stable, iii) the reference wind data are reliable, iv) the surrounding terrain (of both sites) is sufficiently gentle and smooth to ensure mostly attached flows, and v) the topographical model inputs are adequate and reliable.

One objective measure of the steepness or ruggedness of the terrain around a site is the so-called ruggedness index or RIX Bowen and Mortensen (1996), defined as the percentage fraction of the terrain within a certain distance from a specific site which is steeper than some critical slope, say 0.3 Wood (1995). This index was proposed as a coarse measure of the extent of flow separation and thereby the extent to which the terrain violates the requirements of linearized flow models like WASP.

The ruggedness index has also been used to develop an orographic performance indicator for WASP-predictions in complex terrain Bowen and Mortensen (1996); Mortensen and Petersen (1998), where the indicator is defined as the difference in the percentage fractions between the predicted and the reference site. This indicator may provide the sign and approximate magnitude of the prediction error for situations where one or both of the sites are situated in terrain well outside the recommended operational envelope.

WAsP is a small-scale model and the domain is on the order of 10×10 km^2.

2.2 Meso-scale modeling

The statistical dynamical approach of regionalization of large-scale climatology (Frey-Buness et al., 1995) is used to calculate the regional surface wind climate with KAMM. The simplifying assumption is made that the regional surface layer climate is determined uniquely by a few parameters of the larger, synoptic scale, and parameters of the surface. This parameter space is decomposed into several representative situations. Numerical simulations of these situations are performed with the meso-scale model. Then, the meso-scale climatology is calculated from the results of the simulations together with the frequency of the typical situations.

Some important parameters for the surface wind climate in mid-latitudes are the strength and direction of the large-scale pressure gradient, or geostrophic wind, the stratification of the atmosphere, also possible persistent inversions (Frank and Petersen, 1998), changes in terrain height, and surface roughness. Near coasts, the difference of the surface temperature between land and sea can be important for the development of sea breezes. For most wind energy purposes in mid-latitudes, when the interest is mainly in the moderate to high winds, the geostrophic wind together with terrain height and roughness are the dominant parameters.

Different methods are used to define the representative situations. Clustering is used e.g. by Adrian et al. (1996) or Mengelkamp et al. (1997). As we combine the meso-scale simulations with WAsP, we employ 12–16 equidistant direction sectors of the geostrophic wind. Each sector is divided in several speed classes of equal frequency per sector. Usually, more speed classes are used in more frequent sectors.

The stratification of the atmosphere does not change as much as the geostrophic wind. Its importance is measured by the inverse Froude number ${\mathrm{F_r}}^{-1} = NL/U$, where N is the Brunt-Vaisala-frequency, L a typical length scale of the terrain, and U a velocity scale. Hence, stratification is more important at low winds. Therefore, the lowest speed classes in a sector are further divided according to the inverse Froude number. Still, all representative situations with geostrophic wind from one sector have approximately the same frequency.

The frequencies of the classes are only approximately the same because they are determined locally for each point of the large-scale analysis, and interpolated to the grid points of the meso-scale simulations. This accounts roughly for inhomogeneities on the larger scale.

As we assume that the geostrophic wind is the most important external parameter for the surface wind, the representative wind classes must be chosen such that the first three moments of the geostrophic wind speed are well resolved by the representative classes. If e.g. a large part of the third moment of the geostrophic wind speed is lost, it cannot be expected that the full power density of the near surface wind will be modeled. This had been a major source of errors in some unsuccessful attempts to simulate the wind climate.

KAMM

The Karlsruhe Atmospheric Mesoscale Model KAMM (Adrian and Fiedler, 1991; Adrian, 1994) is a three–dimensional, non-hydrostatic atmospheric meso-scale model which assumes non–divergent wind fields in order not to simulate sound waves. Sub-grid scale fluxes are parameterized using a mixing–length model with stability dependent turbulent

diffusion coefficients in stably stratified flow, and a non-local closure for the convective mixed layer Degrazia (1989).

Spatial derivatives are calculated in the model by centered differences using a non-staggered grid. KAMM employs a stretched vertical coordinate which is terrain following at the surface. The model top is at constant height. Therefore, the height above the surface of the grid levels is less above mountain summits than over the sea. Advection is calculated using a flux–corrected–transport–algorithm (Hugelmann, 1988).

Lateral boundary conditions assume zero gradients normal to the side on inflow boundaries, and on outflow boundaries the radiative condition of Orlanski (1976) allows signals to pass out of the model domain without reflections. Gravity waves can penetrate the upper boundary outward using the boundary condition of Klemp and Durran (1983).

The atmospheric model can be coupled to a soil-vegetation model by Schädler (1990); Schädler et al. (1990). However, in the most simulations the model was only run in a semi-stationary state. Then, no soil model is employed. The soil temperature is kept constant.

Simulations with KAMM

The model is initialized from a hydrostatic, geostrophic basic state. In time the flow adapts to the topography. Often the model is initialized with a vertical profile of the geostrophic wind and potential temperature.

For the numerical wind atlas the model is run mainly with stationary forcing, i.e. without radiation. The soil and water surface temperature are given by the difference to the initial air temperature at the surface. Separate values are used for water and land.

Simulations were run on the Fujitsu VX1 super computer of the Danish Supercomputing Centre UNI-C and the IBM RS/6000 computer of Risø National Laboratory.

2.3 Combination of KAMM and WAsP

The meso-scale modeling cannot resolve terrain features below the grid size of the simulations. This shall be done using the small-scale model WAsP.

The combination of KAMM and WAsP is illustrated in Figure 2. A wind atlas file is calculated from the simulations very much like from real data (see Ch. 8 of Troen and Petersen, 1989). The simulated wind is corrected for roughness changes and orographic perturbations on the KAMM grid as in WAsP. The orographic correction is calculated for neutrally stratified, non-rotating flow. Stratification rotation effects are not accounted for in WAsP. Therefore, they must remain in the “cleaned” data like they remain in “cleaned” observations. The roughness change model of Sempreviva et al. (1990) is used to calculate perturbations relative to an upstream roughness which is determined as in WAsP. The upstream roughness is used to transform the “cleaned” wind to the roughness classes of a wind atlas file using the geostrophic drag law (see e.g. Blackadar and Tennekes, 1968).

Extra care must be taken to sample the simulated wind in several wind direction sectors, which is required for wind atlas files. The geostrophic wind classes have a width of some tens of degrees. Hence, on average, a simulated surface wind represents a sector of the same width. If it falls near the boundary of a sector of the wind atlas direction classes, it must be accounted for in both sectors of the wind atlas. Therefore, each simulated wind is split up in a number of wind vectors; typically in 5 values. The split-up winds are obtained by interpolation with the surface wind from the neighboring geostrophic wind class which is “most similar” to the geostrophic wind class which is split. The “most similar” wind class is the one in which the inverse Froude number, determined from the

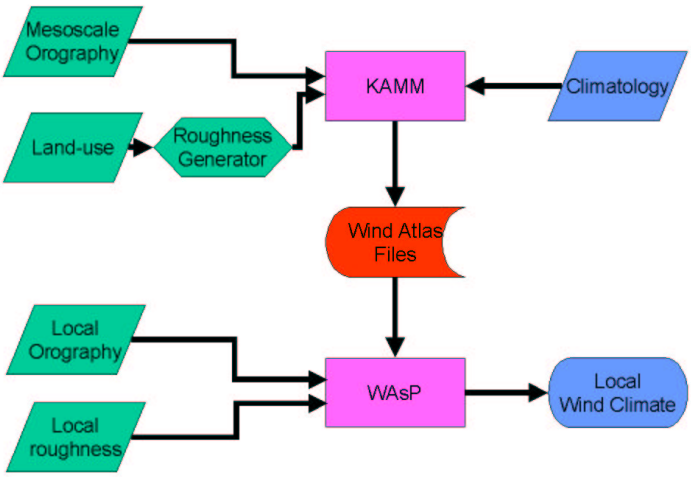

Figure 2. The combination of KAMM and WASP to calculate the local wind climate.

geostrophic wind and the mean stratification, is closest to the inverse Froude number of the split-up geostrophic wind class. The neighboring surface wind is also scaled to the same geostrophic speed with the help of the geostrophic drag law before the interpolation is done. After the simulated winds have been split up, there are enough values (¿500) to calculate frequencies and fit Weibull distributions for different sectors.

Slightly different ways of calculating wind atlas files were tested. The method described above yielded the best results.

The models used in the “cleaning” of the simulated wind used several parameters like WASP. Usually, the standard values of WASP are employed. Some tests were made with different parameter values. In particular, the roughness change model of WASP does not totally eliminate simulated wind speed differences at big roughness changes as along coasts. Obviously, KAMM and WASP model these situations differently. Different parameter values could diminish the differences somewhat. However, the changes are not big and there is no general improvement of the results.

3 Data

3.1 Topography

WASP uses maps which contain lines of constant height and/or roughness change lines. A roughness change line has two values associated with it: The surface roughness length to the right and to the left of the line. The maps can be generated by digitization of topographic maps or exported and reformatted from GIS data sets. The resolution can vary from very high in areas with complicated topography to low in smooth, homogeneous terrain.

KAMM needs grid maps with a constant grid spacing. The data sets used to generate them are described below.

Orography

Terrain heights for the meso-scale simulations are derived from the GTOPO30 global data base (USGS EROS Data Center, 2000a), which has a horizontal resolution of 30 arc seconds, i.e. lless than one kilometer. Figure 3 shows the orography of Denmark given by this data set.

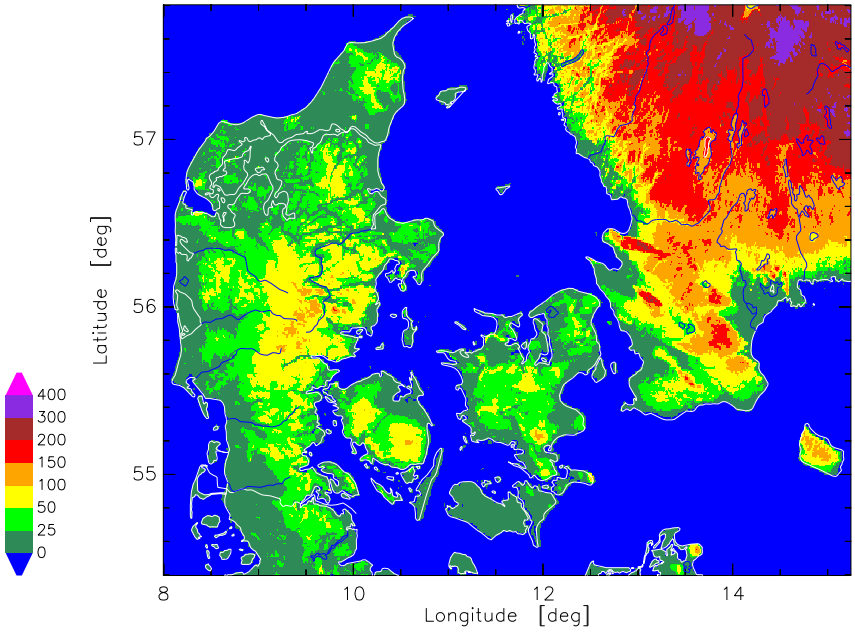

Figure 3. Terrain height of Denmark from the GTOPO30 data base.

The original heights are averaged with a weak Gaussian filter to a 10 km, 5 km, and 2.5 km grid. In order to allow the free propagation of gravity waves out of the modeling domain, the three grid points next to a boundary must have the same height.

Surface roughness

The roughness length of land surfaces is derived from the Global Land Cover Characterization (GLCC) data base (USGS EROS Data Center, 2000b) using the classification of the US Geological Service. It is shown in Table 1 together with assigned roughness lengths. Some roughness values are different for some regions. The classification is derived from AVHRR data. It has a resolution of 1 km^2 in Lambert Azimuth Equal Area projection.

A roughness length z_0 is assigned to each land use class. The coordinates are transformed from the Lambert Azimuth Equal Area projection to the system used in KAMM (UTM, Irish National Grid). Then $\log z_0$ is averaged to the grid size of the simulation to obtain roughness maps for KAMM.

The CORINE land-use database (CORINE = Coordination of Information on the Environment) of the European Community was available for Portugal and Galicia. It has a much higher resolution, and we think it is more accurate. Therefore, it was used for that region.

The roughness length of the water surfaces is calculated from the friction velocity using Charnock's relation (Charnock, 1955). This predicts increasing roughness with increas-

Table 1. The classes of the US Geological Service, which occur in the GLCC data base, and the assigned roughness length z_0.

z_0 cm	class	description
40	100	Urban and Built-Up Land
10	211	Dryland Cropland and Pasture
10	212	Irrigated Cropland and Pasture
10	213	Mixed Dryland/Irrigated Cropland and Pasture
7	280	Cropland/Grassland Mosaic
15	290	Cropland/Woodland Mosaic
5	311	Grassland
7	321	Shrubland
6	330	Mixed Shrubland/Grassland
7	332	Savanna
40	411	Deciduous Broadleaf Forest
40	412	Deciduous Needleleaf Forest
50	421	Evergreen Broadleaf Forest
50	422	Evergreen Needleleaf Forest
40	430	Mixed Forest
0.02	500	Water Bodies
03	620	Herbaceous Wetland
10	610	Wooded Wetland
02	770	Barren or Sparsely Vegetated
05	820	Herbaceous Tundra
15	810	Wooded Tundra
10	850	Mixed Tundra
3	830	Bare Ground Tundra
0.1	900	Snow or Ice

ing wind speed. However, for low wind speeds the roughness increases with decreasing speed. This is described using the roughness length for a smooth surface following Smith (1988). Frank et al. (2000) showed that a fetch-dependent sea surface roughness description is not important for simulation of mean wind speed or mean energy flux density.

3.2 Atmospheric data

The large-scale forcing is determined from several years of the data from the NCEP/NCAR-reanalysis for (Kalnay et al., 1996). In most cases the geopotential height of the 1000, 850, 700, and 500 hPa level and temperature and humidity at 850 and 500 hPa are used. The data is inter- and extrapolated to constant height above sea level and a geostrophic wind is calculated at these heights.

Representative classes of geostrophic winds and stratification are determined from the reanalysis data set. A reference level – surface or ca. 1500 m – is chosen. The geostrophic wind at reference height is sorted in several (typically 16) sectors and several speed classes per sector. The classes with the lowest speed can be further separated in stability classes based on a Froude number with the temperature difference between the surface and next level above the surface. The frequency of the classes in one sector is

approximately the same except for the lowest and highest speed class. These have lower frequencies in order to get a better representation of higher moments of the wind speed distribution. Approximately 150 classes are chosen for a region.

The geostrophic wind is not homogeneous over the modeling domains. Therefore, the frequency of the classes is determined for several points of the large scale analysis, which has a resolution of $2.5°$. For each grid point of the meso-scale simulations the local frequency distribution is calculated by linear interpolation between the known frequencies. This accounts at least partially for horizontal inhomogeneities of the mean geostrophic wind.

The geostrophic wind used for the classification is calculated with one constant Coriolis parameter for a model region because KAMM employs a constant Coriolis parameter. The large-scale forcing for KAMM is an external pressure gradient, which is expressed through a geostrophic wind. The variation of the Coriolis parameter is small. Still, in can change the direction of the gradient of the geostrophic wind because it is weak.

4 The Effect of Map Diameters on Wind Atlas Data

4.1 Method

A major objective of the project was to find out, how the horizontal grid resolution of the meso-scale model KAMM effects the simulated wind atlas. In this context it is interesting to investigate, how important the size of the maps is for a wind atlas calculated with WASP from simulations. Therefore, WASP was run several times for a number of stations using maps of different size. The mean speed, energy flux density, annual energy production, mean direction, Weibull shape parameter, etc. of the wind atlas data was drawn as a function of map diameter.

To avoid any preferred axis the clipped maps were circular with the observation site in the center. Only the line segments within diameters of 2.5, 5, 10, and 20 km were taken. This is illustrated in Figure 4 for the mast at Risø. Circles indicating the extend of the clipped maps are shown overlaid on top of the original map

The main parameters affected by the size of the maps are the orographic speed-up on hills or valleys, and the upstream roughness. As WASP is a neutrally stratified small-scale model the orographic speed-up depends mainly on hills with a half-width of less than a few kilometers. Therefore, almost no effect can be expected for sites in Denmark.

The upstream roughness (Chapter 8.3 of Troen and Petersen, 1989) is used to transform the observed wind to different roughness classes of a wind atlas. The decay length for the magnitude of roughness changes in WASP is 10 km. Therefore, small maps can result in wrong upstream roughness values in WASP. For example, in the circular map with diameter 10 km WASP must assume that there is only water in the sector around $300°$. This would yield an underestimation of the wind in the wind atlas from that sector. In reality the surface friction of the upstream land has reduced the wind speed compared to pure over-water conditions.

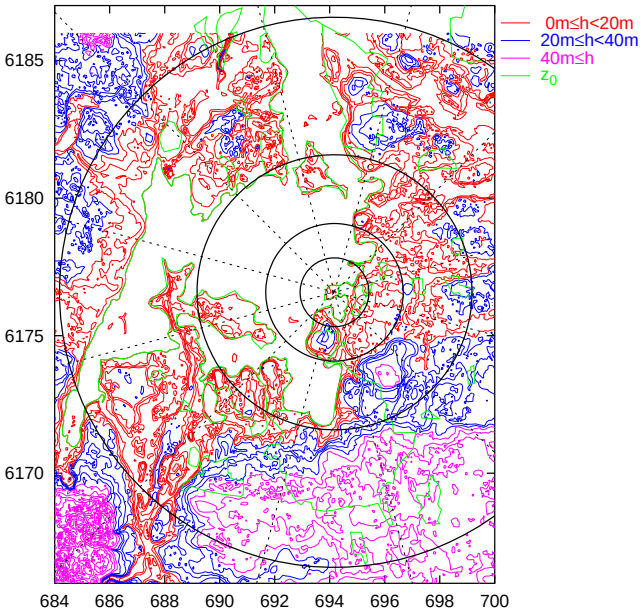

Figure 4. WASP map of Risø. Circles with diameters 2.5, 5, 10, and 20 km are drawn around the position of the mast. Roughness change lines are green.

4.2 Results of varying the map diameters

We shall concentrate here on the wind atlas values at 50 m height above a surface with roughness 3 cm. This is close to typical heights of many modern turbines and 3 cm roughness represents a good site on land.

Figures 5 and 6 show the energy flux density, E, and annual energy production, AEP, as functions of map diameter for sites in Denmark and Ireland. The important result is that even using maps with diameters 10 km, i.e. 5 km distance to a site, errors greater than 15 % in energy flux density, and greater than 10 % in annual energy production can occur in wind atlas data. At sites within a few kilometers from a coast line, which lies upwind in the dominant wind direction, it is very important to include the coast line in the map. Examples are the stations Klemensker Ø on Bornholm, and Tystofte on Zealand. Comparing Figures 5, 6 with Figure 7 it can be recognized, that to a great extent the mean energy of the wind atlas data follows the upstream roughness used by WASP. The strength of the variation of E or AEP is not directly proportional to the variation of z_0. This depends also on how much of the total energy is concentrated in the sector with the highest energy flux density.

The ruggedness index, RIX, is zero or small for almost all stations in Denmark and Ireland. Consequently, the orographic speed-up is relatively small. The orographic speed-up in WASP acts on smaller scales than roughness change effects. Good examples are the stations Corrie Mountain, Kilronan Mountain, or Mount Eagle in Ireland. If the map gets so small that it does not encompass the full mountain, the orographic speed-up can be seriously underestimated. However, already for map diameters of 5 km the errors for the orographic speed are less than 5 % for almost all the stations in Denmark and Ireland.

The Weibull shape parameter k does not change much with varying map size. If the map diameter is 10 km or greater the mean wind direction deviates less than 5 degrees from the value obtained with the full map.

The sites in the mountains of Portugal are quite different from the sites in Denmark or

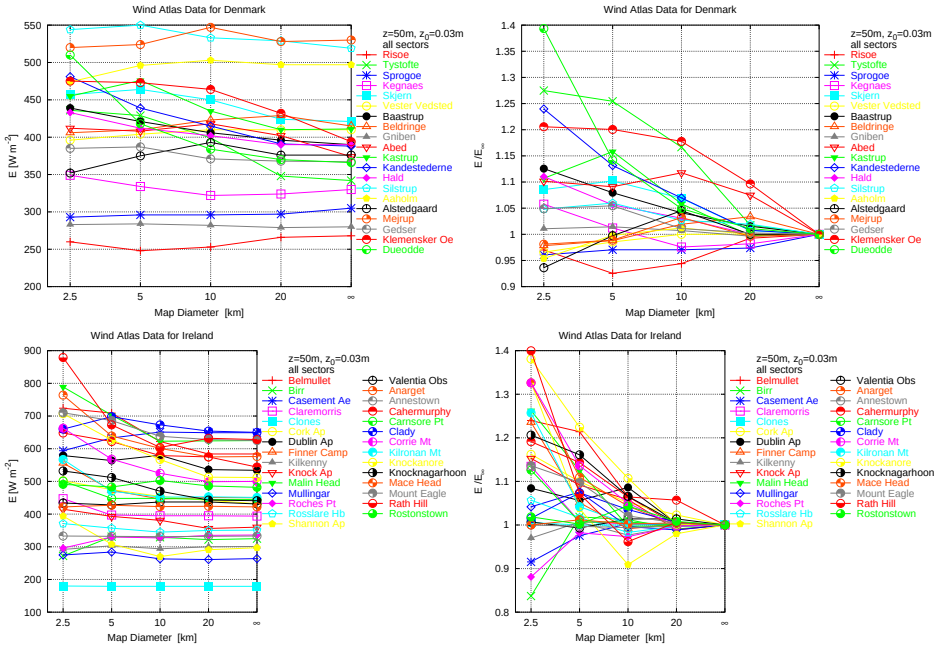

Figure 5. Energy flux density, E, at 50 m above 3 cm roughness as a function of map diameter. The symbol ∞ represents the full, original map. The top row shows stations in Denmark, the bottom row stations in Ireland. The left column shows the absolute values in $W\,m^{-2}$, and the right column the relative changes, E_D/E_∞.

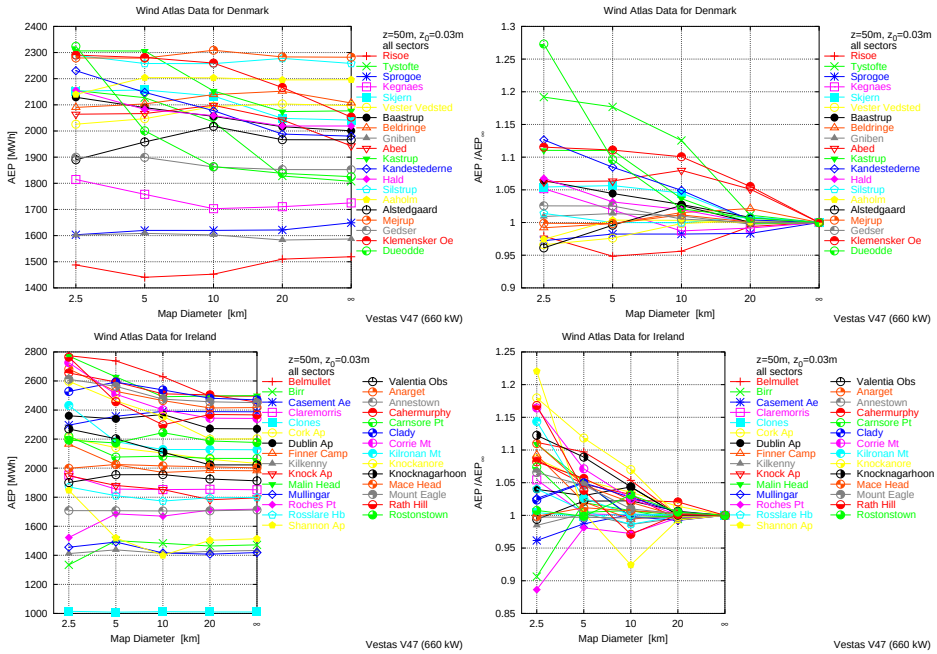

Figure 6. Annual energy production of a Vestas V47 (660 kW) turbine if had a hub height of 50 m above a flat surface with roughness length 3 cm. The top row shows stations in Denmark, the bottom row stations in Ireland. The left column shows the absolute values in MWh, and the right column the relative changes, AEP_D/AEP_∞.

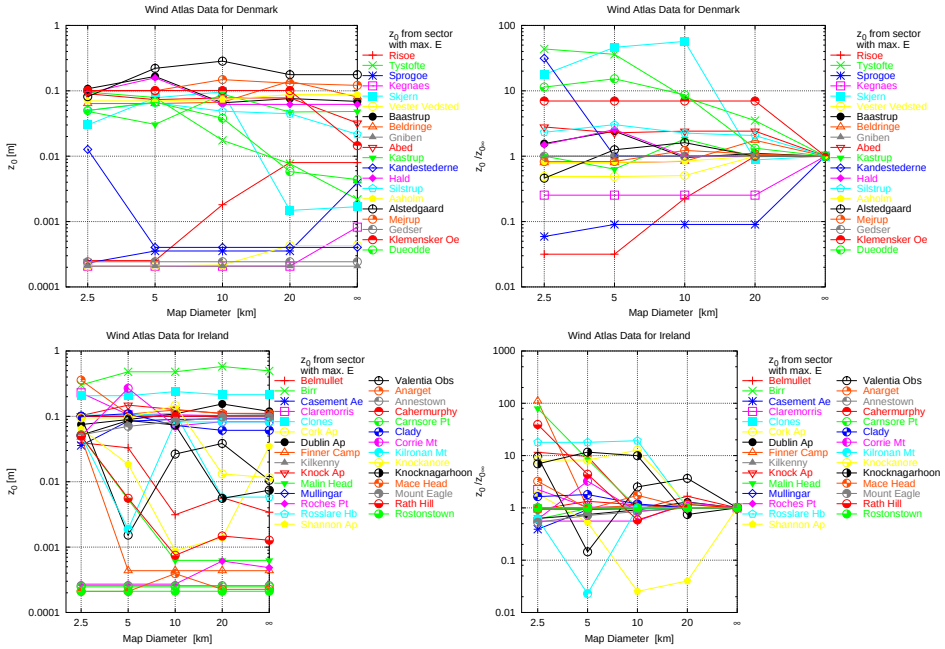

Figure 7. The upstream roughness length in the sector where most of the energy flux density is observed as a function of map diameter. The top row shows stations in Denmark, the bottom row stations in Ireland. The left column shows the absolute values in m, and the right column the relative changes, $z_{0D}/z_{0\infty}$.

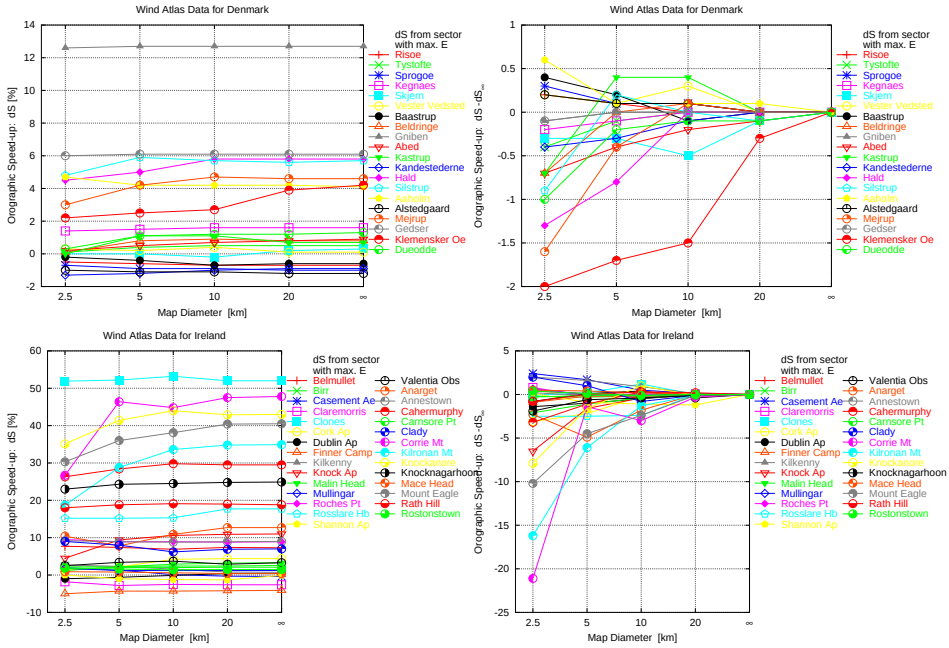

Figure 8. Orographic speed-up in the sector where most of the energy flux density is observed as a function of map diameter. The top row shows stations in Denmark, the bottom row stations in Ireland. The left column shows the speed-up in %, and the right column the difference to the value for the full map, $\Delta S_D - \Delta S_\infty$.

Ireland as indicated by their ruggedness index (Table 2). Only the station Murtosa, which lies on the flat coast, has a RIX-value zero. Average values up to 30 are reached. Even $RIX = 49$ is reached in individual sectors. The ruggedness index depends somewhat on the size of the area for which it is calculated. For the steep sites with high RIX-values, it tends to increase with decreasing radius, whereas it tends to decrease with decreasing radius for the sites with RIX approximately less than 10.

Table 2. Ruggedness indices, RIX, for stations in Portugal.

Name	avg.	sector [deg]											
	RIX	0	30	60	90	120	150	180	210	240	270	300	330
Murtosa	0	0	0	0	0	0	0	0	0	0	0	0	0
Afonsim	11	0	6	10	22	34	22	21	17	2	0	0	0
Lamas	4	2	1	0	1	8	18	17	2	0	1	1	2
Penude	10	4	3	3	15	19	37	26	6	1	4	3	4
Aveloso	13	2	5	4	2	12	14	13	19	16	23	26	19
Pena	25	19	37	30	29	30	29	16	10	26	26	28	17
Drave	28	37	13	14	22	36	34	35	28	35	25	30	29
Arada	16	16	29	34	35	17	3	0	8	4	17	19	14
Adaufe	8	10	13	20	18	18	13	0	3	1	2	2	1
Castanheira	8	1	1	0	1	5	19	12	7	8	23	13	10
Senhora de Moreira	30	36	3	13	26	33	35	25	24	33	32	48	49
Marao	28	34	35	22	18	39	32	21	29	20	17	27	44
Lagoa de Joao	1	4	0	1	3	6	0	0	0	0	0	0	2

The dependence of energy flux density, E, and annual energy production, AEP, on map diameter for the Portuguese stations is shown in Figure 9. Most maps cover an area of only 12×8 km^2. Therefore, diameters from 1 km to 10 km are chosen. Obviously, maps with diameters of 5 km are far to small to get a reliable estimate of the mean energy flux density. Errors greater than 10 % must be expected in this type of terrain.

For most sites the orographic speed-up is seriously underestimated when using small maps (Figure 10). For maps with diameters 5 km, the error of the mean wind speed can be over 5 %. The errors might be even greater if bigger maps were available because there might be weak speed-ups at greater scales than the total map size. Errors in mean wind direction are less than 3°. The Weibull shape parameter, k, differs by less than 3 % from the value with the full map.

5 Errors

Before presenting the results for each country we shall comment on the expected errors of the analysis. First, we summarize the errors of WASP, and then we mention errors of using KAMM and WASP for wind energy assessment.

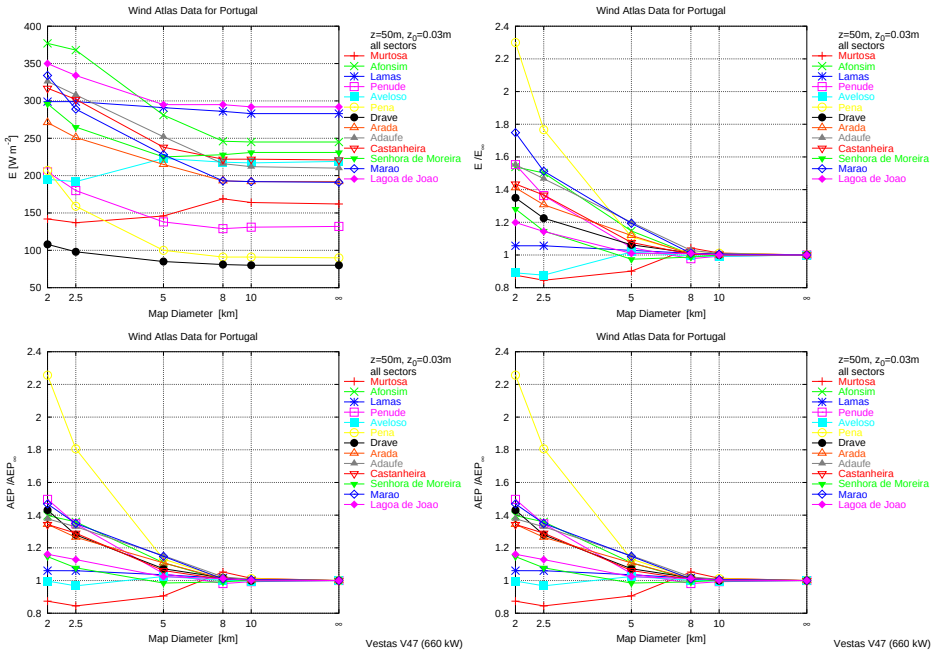

Figure 9. Energy flux density (top) and annual energy production of a Vestas V47 (660 kW) turbine (bottom) for sites in Portugal from wind atlas data at 50 m above a flat surface with roughness length 3 cm.

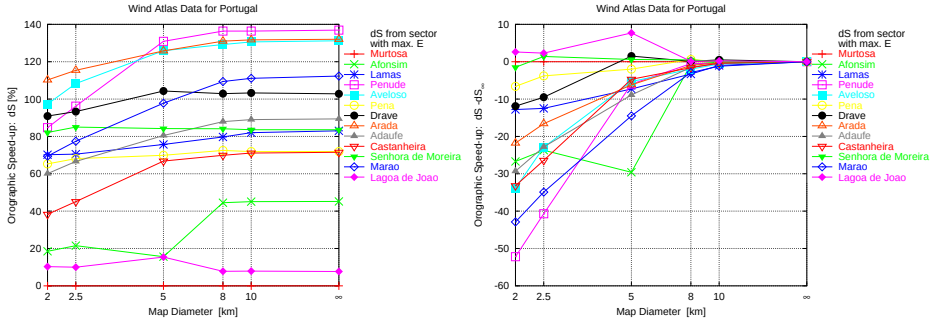

Figure 10. Orographic speed-up in the sector where most of the energy flux density is observed as a function of map diameter at sites in Portugal. The right shows the difference to the value for the total map, $\Delta S_D - \Delta S_\infty$.

5.1 Errors of WASP

WASP is a linear flow model for neutrally stratified flow. It does not account for Coriolis accelerations. Hence, it can only simulate flow over weak to moderately steep terrain on scales of less than a few kilometers distance. Considering the simplifications made to the physics it is astonishing, how well the model can be applied in many situations.

WASP is used all over world for wind resource assessment. Typical errors of the annual energy prediction of wind turbines are about 10 %. In complex terrain as e.g. mountains larger errors must be expected.

The so-called self prediction of a station is usually very accurate, with errors of less than 2 %. It is the prediction for exactly the same location where the original data was measured using the wind atlas generated from it.

5.2 Errors of the KAMM/WASP method

Most errors of KAMM are mentioned in combination with errors of the method of mesoscale modeling of the wind energy. One aspect not mentioned below is the closure model for the turbulent fluxes. The parameterization works well, but it cannot be perfect in all flow situations.

There are many assumptions and simplifications in representing the natural wind climate by a few, though more than 100, simulations. Sources for errors of this analysis are listed below:

- The stratification of the atmospheric surface layer is important for the shape of the wind profile. The temperature difference between air and the surface was estimated from the reanalysis data. Also, the stability model of WASP Troen and Petersen (1989) can be used to calculate climatological mean wind profiles.
- Neglect of unstationary flow fields, e.g. atmospheric fronts, and daily variations, e.g. sea breezes. Sea breezes could be important for the coastal areas of Portugal. Unstationary flow fields are much more important for extreme winds than for mean winds.
- Some simulations did not reach an exactly stationary state. This is mainly a problem over water, where the turbulence is very low. Simulations with weak geostrophic wind, i.e. weak forcing, were run for a longer time to reduce this error.
- Representativity of the geostrophic wind classes. The representativity decreases for higher moments of the distribution of the geostrophic wind. Also, differences between the analysis period of the large-scale data and the observations period at specific sites will introduce apparent errors.
- Different atmospheric mean stratification and baroclinicity. The mean stratification is important for the flow over and around mountains. Usually, it does not change very much in the free atmosphere. The baroclinicity is the variation of the geostrophic wind with height. This is important for Portugal. It was introduced via non-constant profiles of the base state in KAMM.
- Errors in the maps. These should be small for the orography. Roughness maps are always more difficult to obtain. The land use classification from the satellite data can contain errors. Also, the assignment of one roughness value to a land use class is only a rough description. As long as the roughness map is not totally wrong, the error should be smaller for wind atlas data than for wind resource calculations.
  An error is introduced by the fact, that the model cannot know the topography outside the simulation domain. Hence, results are less reliable at grid points close to boundaries than in the center of the domain.
- Inhomogeneities of the large scale geostrophic forcing. This is partially accounted for by using local frequencies of the classes.

When simulation results are compared with observations differences can appear because of periods with missing observations, or when the forcing data for KAMM covers a different period than the observations. When several years of observations are available these differences can be expected to be small.

6 The Numerical Wind Atlas for Denmark

6.1 Topography for Denmark

The topography of Denmark was derived from the GTOPO30 and GLCC data bases as described in section 3.1. A summary is given in Table 3. Height maps are shown in Figure 11, and roughness maps in Figure 12. The maps include a small part of southern Norway as it might influence the flow field in the northwest of Denmark.

Table 3. Maximum terrain height, h, and roughness length, z_0, average roughness lengths, $\langle z_0 \rangle$, and fraction of land areas for the maps of Denmark used by KAMM.

Δx	10 km	5 km	2.5 km	
Grid size	45×54	80×100	160×200	points
Max. h	324	336	336	m
Max. z_0	0.50	0.50	0.50	m
$\langle z_0 \rangle$	0.062	0.042	0.041	m
$\langle z_{0\,land} \rangle$	0.148	0.142	0.142	m
Fraction land	52	46	46	%

The maps have slightly different size. Still, the average roughness of the different maps are similar (Table 3). The 10 km grid map is larger than the other two. It contains more land areas. Therefore, its average roughness is greater.

The grid of KAMM had 25 levels from the surface to a height of 4000 m. The lowest grid levels where at 15, 43, 84, 138 m a.g.l. for a grid point at sea level.

6.2 Geostrophic wind over Denmark

The large-scale forcing was determined from 10 years of the geopotential height of the 1000, 850, 700, and 500 hPa level and temperature and humidity at 850 and 500 hPa of the NCEP/NCAR-reanalysis for 1987-1996 (Kalnay et al., 1996). The geostrophic wind at 850 hPa and a Froude number of the mean stratification determined the classes. The data was inter- and extrapolated to the heights 0, 1000, and 5000 m.

Representative classes of geostrophic winds and stratification were determined from the reanalysis data set. The geostrophic wind was sorted in 16 sectors and with 6–11 speed classes per sector. The classes with the lowest speed were further separated in 1–3 stability classes based on a Froude number with the temperature difference between 0 m and 1000 m. The classification resulted in a total of 146 classes.

The geostrophic wind and the frequency of the classes is shown in Figure 13 for the point 11.25° W, 56.25° N in the Kattegat.

The variation of the geostrophic wind across Denmark is shown in Figure 14. Mainly the geostrophic wind decreases towards east. The geostrophic wind shown in Figure 14 is calculated with a constant Coriolis parameter corresponding to latitude 56.25° N because KAMM uses the f-plane approximation. The large-scale forcing for KAMM is an external pressure gradient, which is expressed through a geostrophic wind. Therefore, Figure 14 must show only the variation of this pressure gradient. This pressure gradient is slightly stronger in NW Denmark than in SW Denmark. When the geostrophic wind were cal-

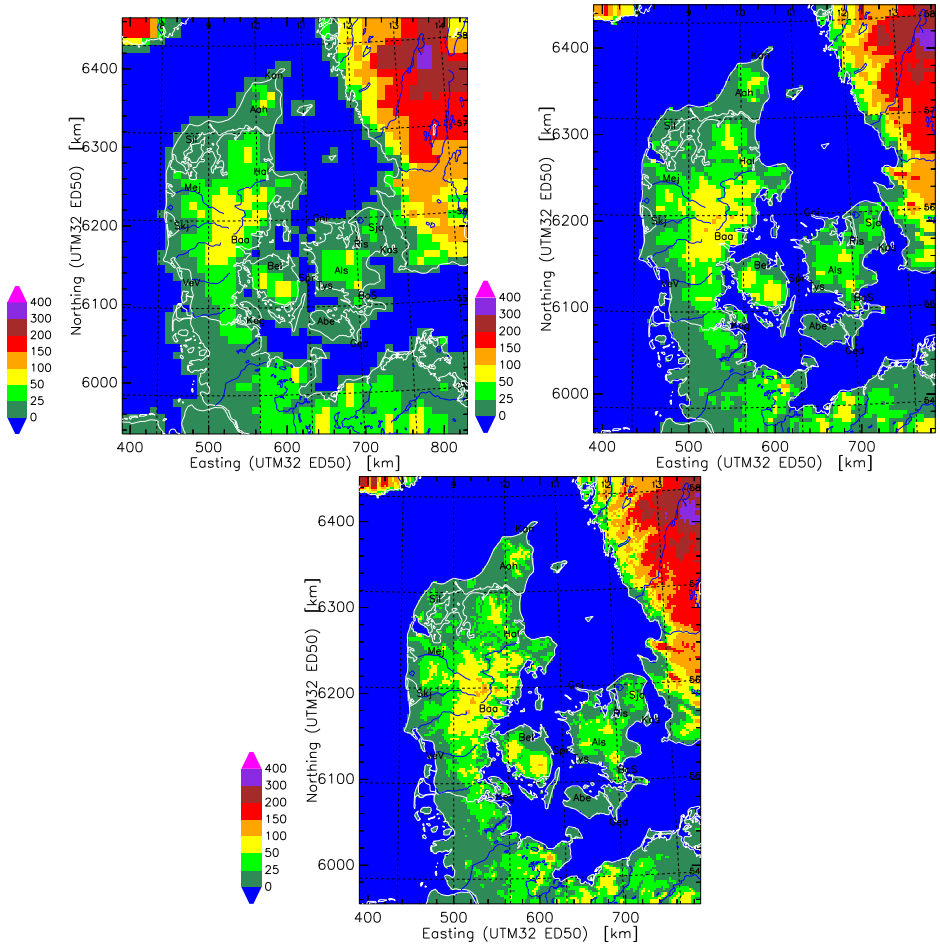

Figure 11. Terrain heights [m] for the 10 km, 5 km, and 2.5 km grid of Denmark. Boundaries and rivers are shown by read and blue lines. The position of observation sites is shown by a code for the station.

culated with varying Coriolis parameter the weak maximum lies in northern Germany in the SW corner of Figure 14.

6.3 Wind resource maps for Denmark

Wind resource maps for Denmark are shown in Figures 15 and 16. The mean speed at 50 m a.g.l. above the roughness grid used for the simulations is shown. The wind speed, or third moment of the wind speed, of each simulation is weighted by the frequency of occurrence of the corresponding geostrophic wind class. The mean energy flux density is calculated with a constant standard air density of 1.225 kg m^{-3} as in WASP.

The main features of these wind resource maps are the difference between sea and land areas. The weakest mean winds are in the big forests in Southern Sweden because their surface roughness is high.

The wind resource maps can be compared with the Wind Resource Map for Denmark (Figure 17, right; Energi- og Miljødata, 1999; Mortensen et al., 1999). It shows the energy flux density at 45 m a.g.l. for the land areas of Denmark. It is based on WASP analyses of observed winds at Danish stations plus the production data of over a thousand wind turbines. The Danish Wind Resource Map is calculated with a grid resolution of 200 m. Therefore, it contains much more detail than the KAMM simulations on the 2500 m grid.

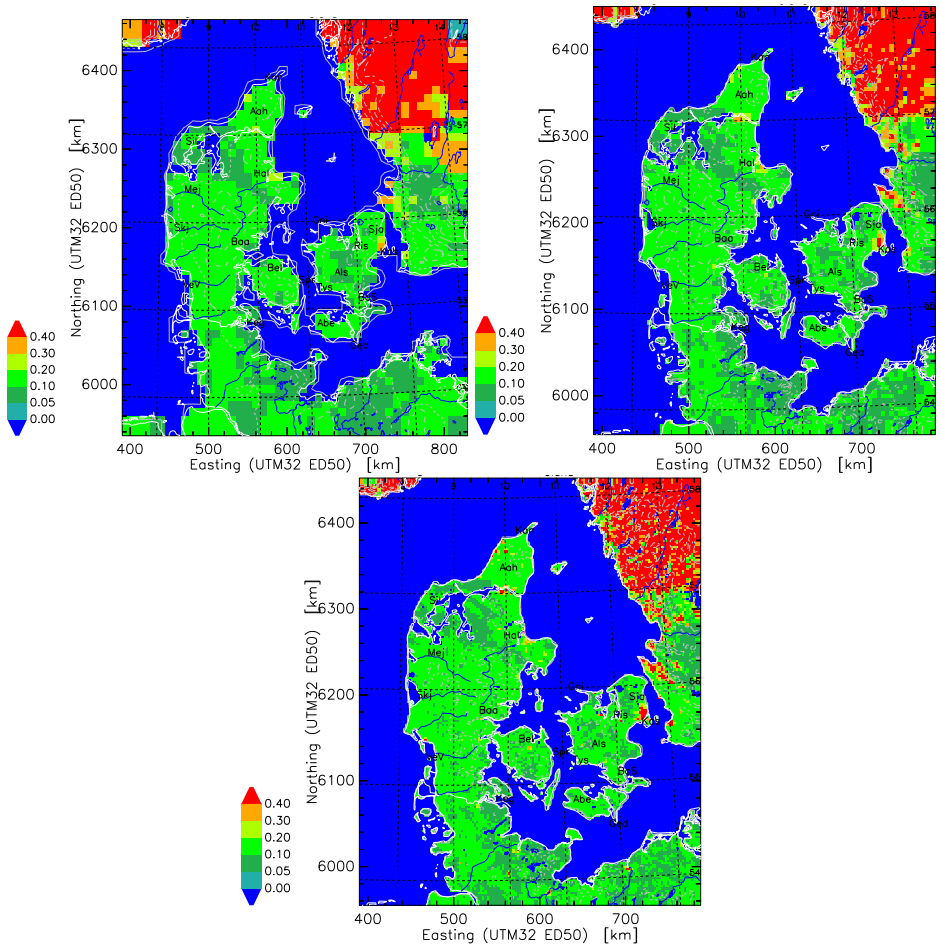

Figure 12. Roughness length [m] for the 10 km, 5 km, and 2.5 km grid of Denmark.

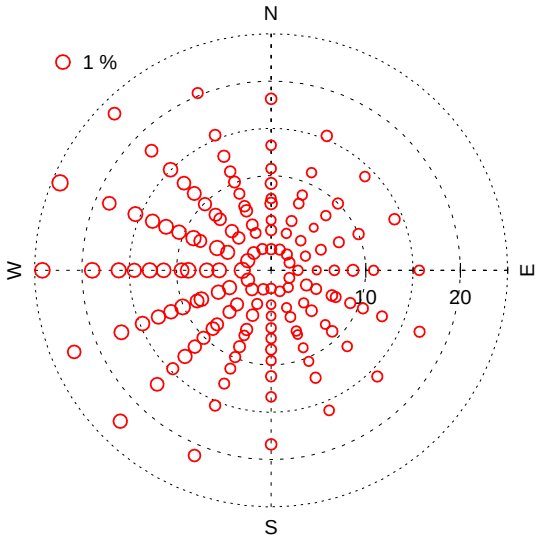

Figure 13. Geostrophic wind at 0 m of the 146 classes, for which simulations were made. The size of the circles is proportional to the frequency at 11.25°E, 56.25°N.

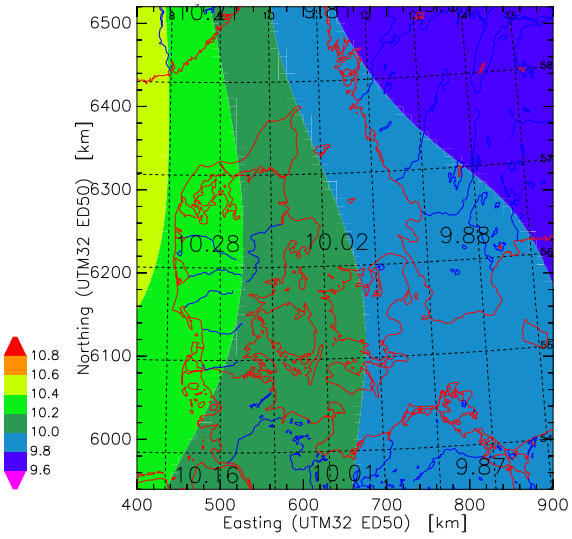

Figure 14. Variation of the geostrophic wind at 1450 m over Denmark

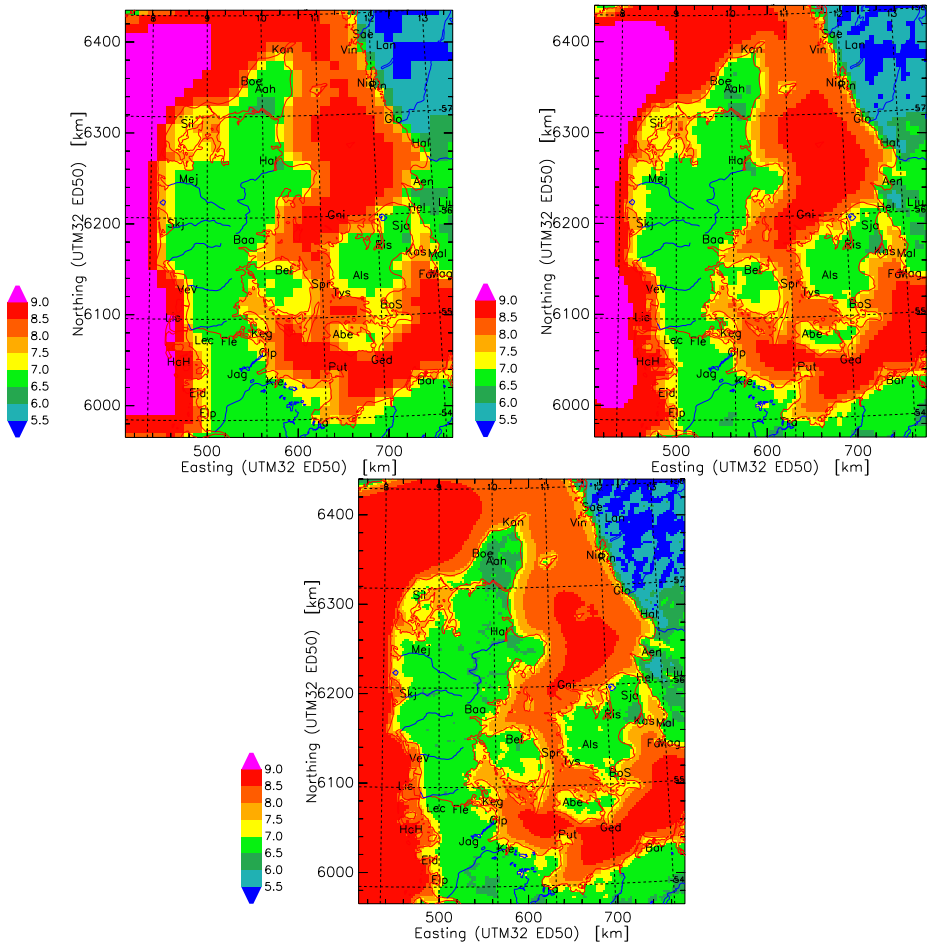

Figure 15. Resource maps of the mean speed, U [m s^{-1}], at 50 m a.g.l. as calculated by KAMM with grid sizes of 10 km (top left), 5 km (top right), and 2.5 km (bottom).

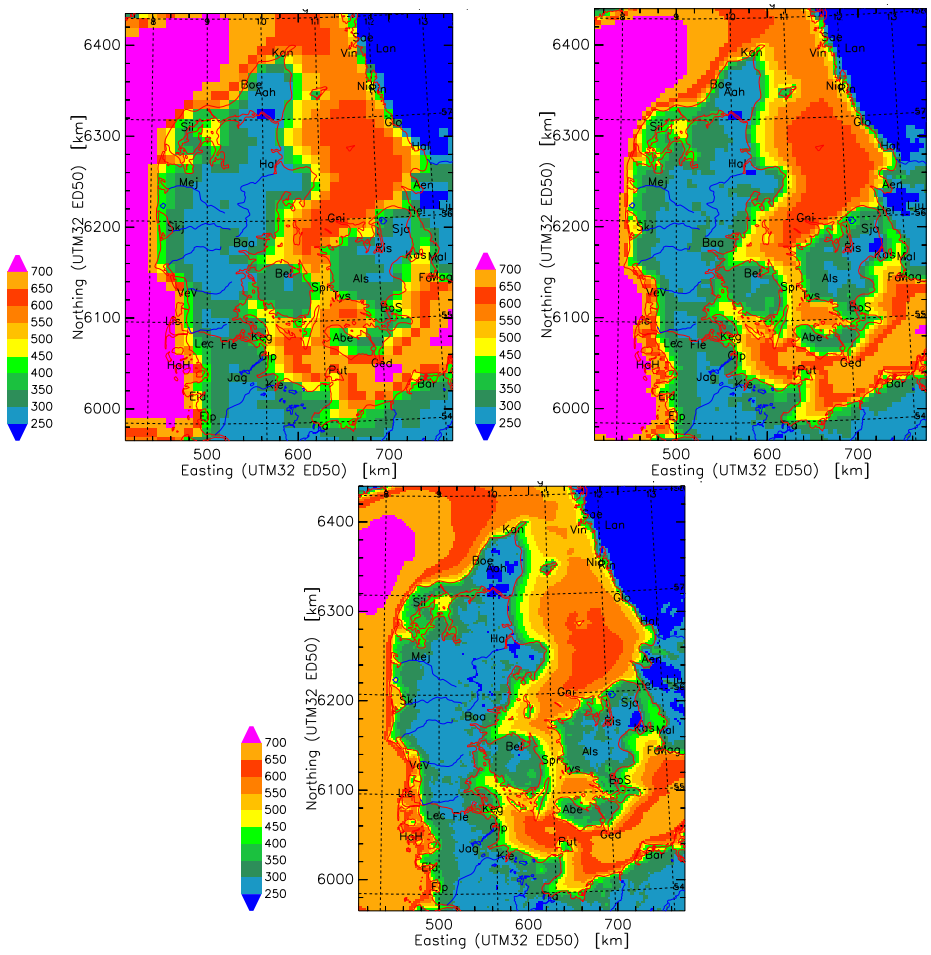

Figure 16. Resource maps of the energy flux density, E [$W\,m^{-2}$], at 50 m a.g.l. as calculated by KAMM.

Still, the overall picture is very similar. Especially, the good sites along the western coasts are clearly visible.

6.4 Wind atlas Maps for Denmark

Wind atlas maps for Denmark are shown in Figures 18 and 19. They show the mean wind speed and energy flux density at 50 m a.g.l. transformed to a plane with a uniform roughness of 3 cm. The main difference to the wind resource maps in Figures 15 and 16 is the reduction of the values over the sea areas. The map is much more uniform as one would expect.

Unfortunately, the coast line is still visible. This reflects mainly the difference of the roughness change models of WASP and KAMM. Minor effects can be stability differences between sea and land which are not accounted for in the roughness change model of WASP.

Also these wind atlas maps are generated slightly differently than wind atlas files (LIB-files) for each grid point, which will be compared with individual stations in the next section. The algorithm uses one mean wind direction over the entire area in order to speed up the calculation of these maps.

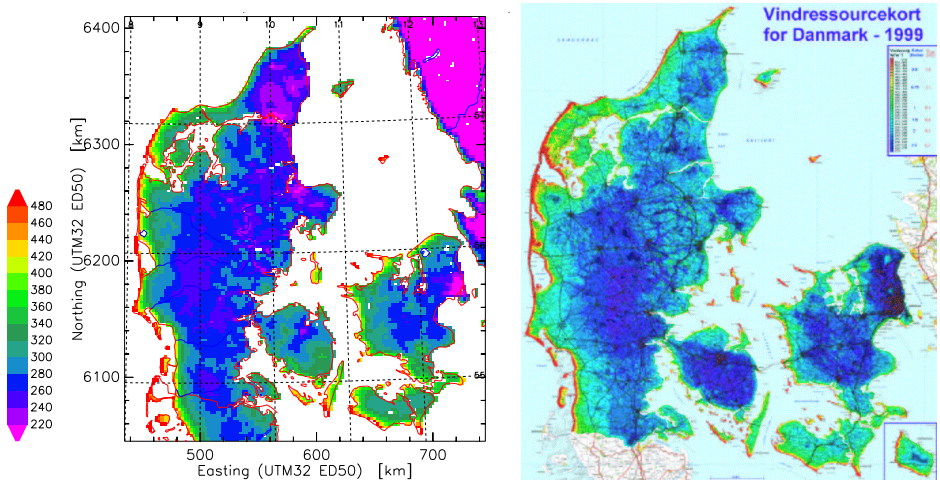

Figure 17. Maps of the energy flux density, E [$W\,m^{-2}$], at 45 m a.g.l. as calculated by KAMM (left) and the Wind Resource Map for Denmark (Energi- og Miljødata, 1999) (right). The resolution is 2.5 km for the KAMM simulations and 200 m for the Wind Resource Map for Denmark.

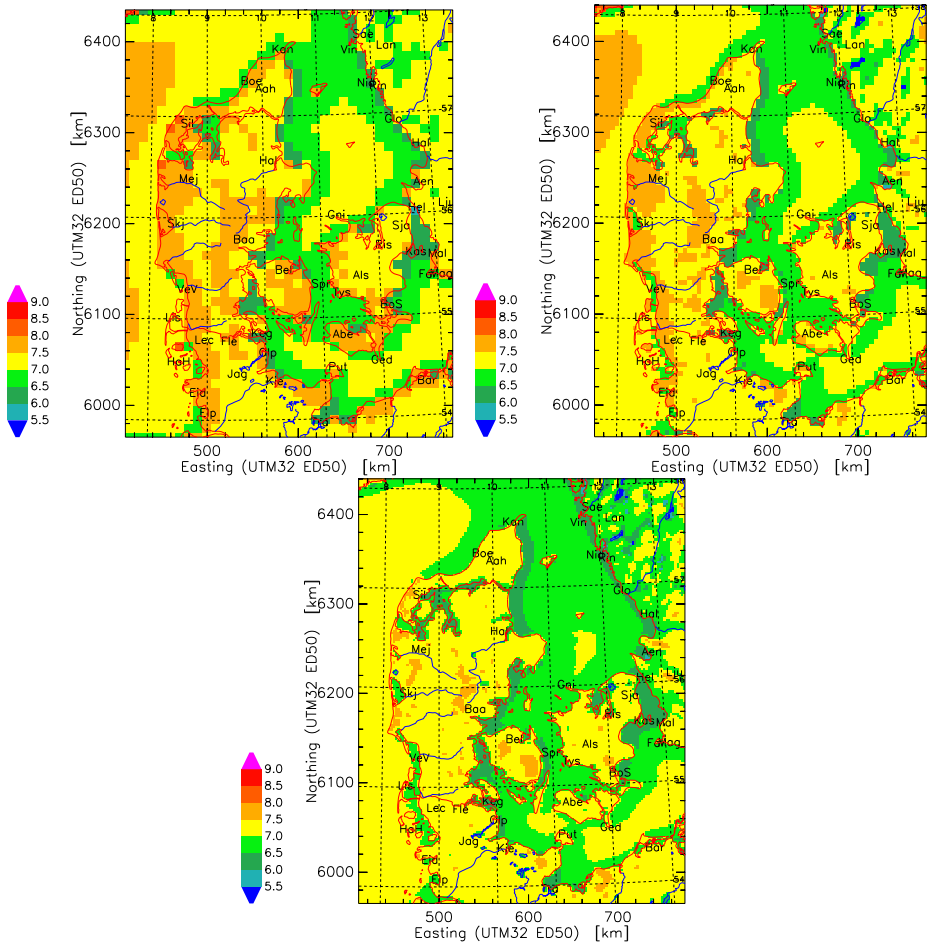

Figure 18. Maps of the mean speed, U [$m\,s^{-1}$], at 50 m a.g.l. above 3 cm roughness calculated by KAMM. These maps can be compared with the resource maps in Figure 15.

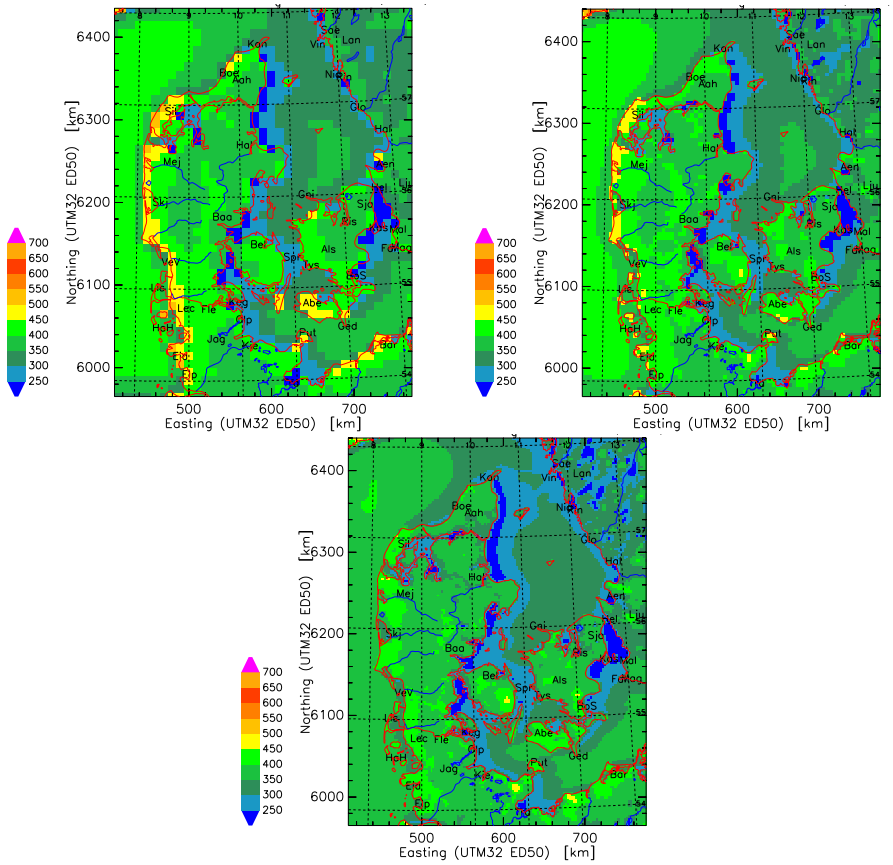

Figure 19. Maps of energy flux density, E [$W\,m^{-2}$], at 50 m a.g.l. above 3 cm roughness calculated by KAMM. These maps can be compared with the resource maps in Figure 16.

6.5 Comparison with observations

The main comparison with observed data is done for the stations used in the analysis of the Danish Wind Resource Map. Wind atlas files are calculated for the nearest grid point and compared with wind atlas data obtained from a WASP analysis of observed data. As the self-prediction of WASP is very accurate, perfect agreement of the wind atlas data would result in very accurate predictions for a site.

The ruggedness index, RIX, is zero for all stations used in the comparison. Therefore, the WASP analysis should be good. At the station Gniben the ruggedness index can reach values above 10 at short distances in the northern and southern sectors. The station lies on a long, narrow peninsula with steep slopes at the northwestern tip of Zealand. The measurement height is 10 m a.g.l. and the site is less than 100 m away from the edges to the north and south. Gniben is one of the stations with least energy flux density. The simulations predict higher values. Perhaps, the corrections applied by WASP are somewhat too high. In summary, the WASP analysis for the stations in Denmark is very reliable.

Comparison are done again for the height of 50 m a.g.l. and roughness length 3 cm because these values are represent good locations and are close to the size of modern wind turbines. Mean speed, wind direction [1], energy flux density, and annual energy production are compared in Figures 20 and 21. The power production is calculated for a Vestas V47 (660 kW) turbine, if it had a hub height of 50 m. Turbines have a cut-in speed where they start energy production and a cut-out speed where they stop in order to reduce the

[1] The direction of the mean vector wind calculated from the wind atlas data

loads on the structure. Hence, the comparison of annual energy production emphasizes the important part of the wind distribution.

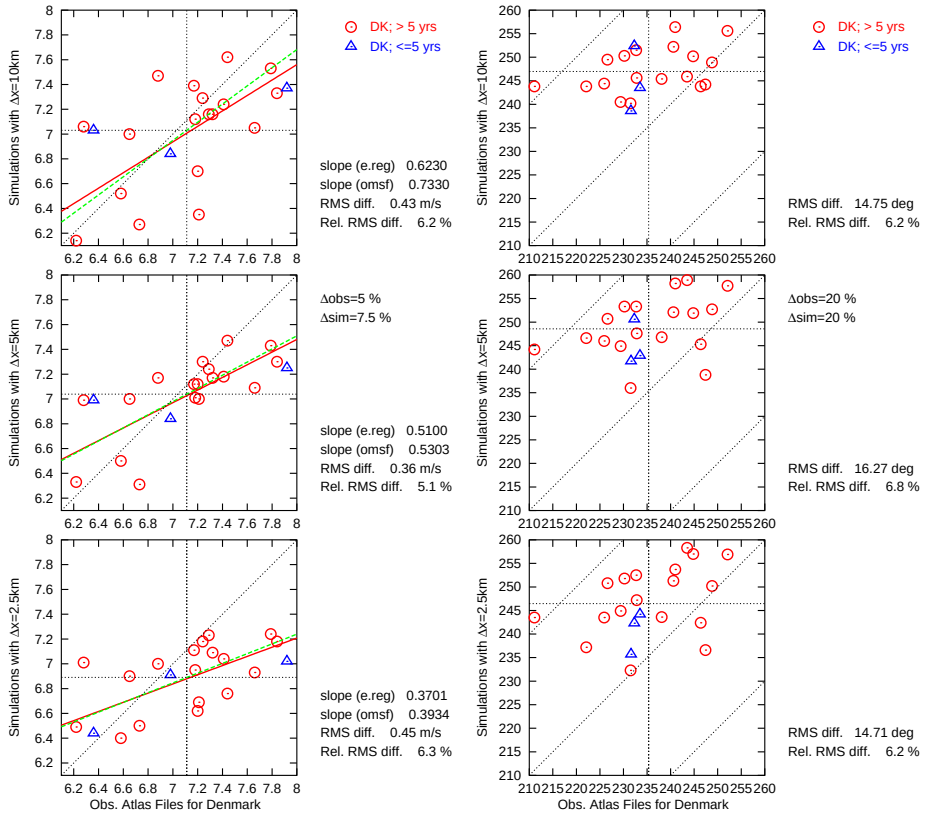

Figure 20. Comparison of wind atlas values derived from observed winds and from simulated winds. Shown are mean speed, U (left), and mean vector wind direction, DD (right), at 50 m a.g.l. above 3 cm roughness.

Figures 20 and 21 show the wind atlas data derived from observations on the abscissa. The value derived from the KAMM/WASP analysis is shown on the ordinate for the three grids with resolution 10 km, 5 km, 2.5 km. Two straight lines are drawn through the data. The dashed, green line is an optimal mean square fit which minimizes the distance orthogonal to the line Kristensen (1999). This assumes equal accuracy for both data sets. The slope of this line is written on the right — slope (omsf) — of each plot.

The red line is a regression line which accounts for errors in both data sets. The assumed errors are written on the right of the central plot: Δobs, Δsim. The slope depends on the ratio of both errors. It was assumed that the error of the KAMM simulations plus WASP analysis is 50 % greater than the error of the WASP analysis of the observed winds. The slope of this regression line — slope (e.reg) — is written above the slope of the optimal mean square fit.

Additionally, the root-mean-square (RMS) value of the difference of wind atlas data from observations analyzed with WASP, U_{OW}, and wind atlas data from KAMM, U_{KA}, are written next to the plots. The relative RMS is the RMS-value of the relative differences $2(U_{OW}-U_{KA})/(U_{OW}+U_{KA})$. The RMS value of the difference emphasizes differences of large values, whereas the relative RMS value emphasizes differences of small values.

The slopes and RMS values can be interpreted as different measures of the quality of the simulations. Ideal predictions and observations would yield a slope of 1 and RMS differences zero.

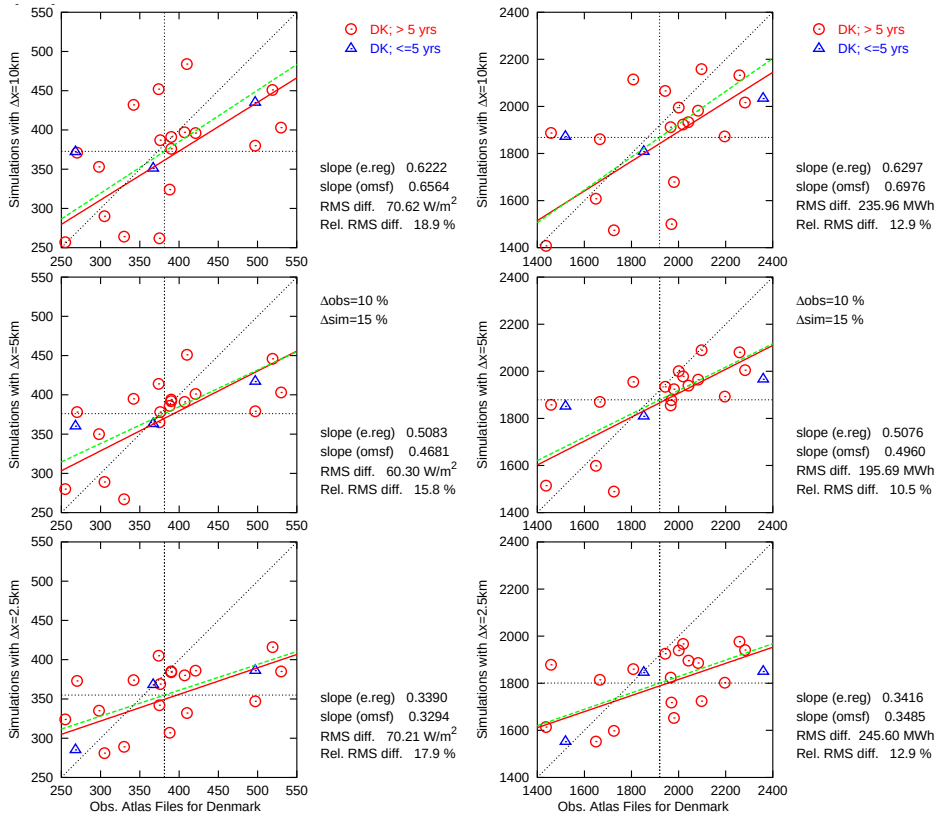

Figure 21. Comparison of wind atlas values derived from observed winds and from simulated winds. Shown are energy flux density, E (left), and annual energy production, AEP (right), at 50 m a.g.l. above 3 cm roughness. The power production is calculated for a Vestas V47 (660 kW) turbine, if it had a hub height of 50 m over a flat site.

The main result is that there is no improvement of the predictions using simulations with higher resolution.

The spread of the points in the plots seems big. However, the RMS differences do not contradict the assumptions on the observation and simulation errors. The error of the difference $y - x$ is the square root of the sum of the square of the errors of x and y. Therefore, if the error of E_{OW} is gaussian distributed with a standard deviation of 10 %, and it is 15 % for E_{KA}, then the RMS value of the difference ΔE is greater than 18 %.

Also, one must remember that the variation of the regional wind climate across Denmark is only small. The uncertainty of the WASP analysis is almost as big as the mean variation.

Another interesting way of assessing the value of the KAMM/WASP analysis is a comparison of simulated values and directly observed values. Figure 22 compares on the left, the simulations of KAMM with the measured mean wind speed. The KAMM values are interpolated from the nearest grid points to the exact position of the sites and to the same observation height. Observation heights range from 8 m a.g.l. to 117 m a.g.l.. No correction for differences of the local roughness and the roughness used in KAMM is made. On the right, wind atlas files were calculated from the simulations. Then a prediction was made with WASP using these wind atlas files. Clearly, the predictions are much better using KAMM *and* WASP

Figure 23 shows the same comparison for the energy flux density with the same result.

The comparison between predictions by KAMM and WASP and the observations is

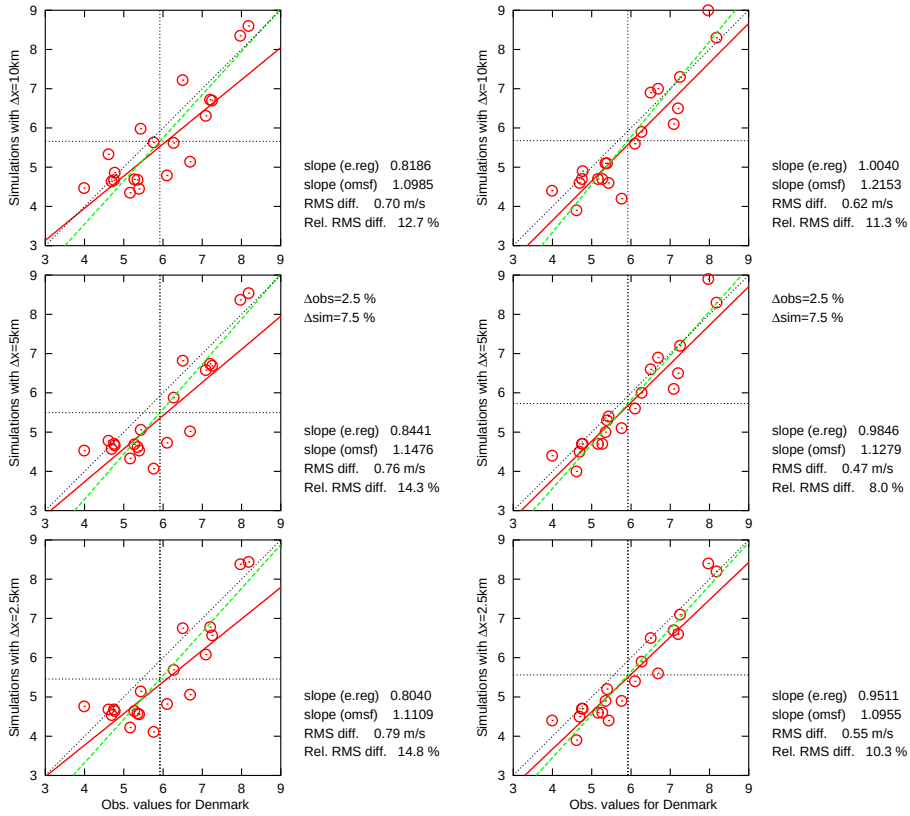

Figure 22. Comparison of the observed mean wind speed at sites in Denmark with predictions using only KAMM (left) and predictions using KAMM and WASP (right). The observation heights range from 10 to 40 m a.g.l..

better when the wind atlas file from the nearest grid point over land is used instead of the nearest grid point, except at very exposed sites like Sprogø Islands or Gedser, where the measurement represent essentially over-water conditions. Then, the RMS of the relative differences of speed, U, are less than 8 % for all grids. For energy flux density, E, they are less than 23.5 %.

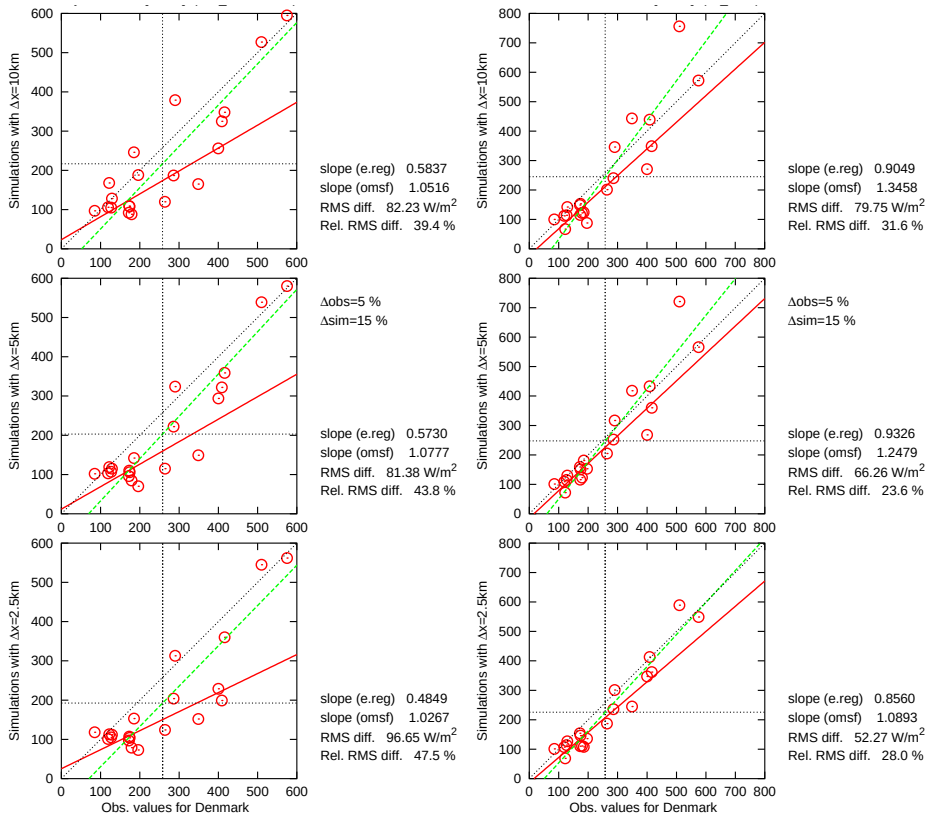

Figure 23. Comparison of the observed energy flux density[3] at sites in Denmark with predictions using only KAMM (left) and predictions using KAMM and WASP (right).

7 The Numerical Wind Atlas for Ireland

7.1 Topography for Ireland

The topography of Ireland was derived from the GTOPO30 and GLCC data bases as described in section 3.1. A summary is given in Table 4. Height maps are shown in Figure 24, and roughness maps in Figure 25. The maps include a small part of British Island as it might influence the flow field in the northeast of Ireland.

Table 4. Maximum terrain height, h, and roughness length, z_0, average roughness lengths, $\langle z_0 \rangle$, and fraction of land areas for the maps of Ireland used by KAMM.

Δx	10 km	5 km	2.5 km	
Grid size	48×54	90×108	180×212	points
Max. h	477	522	698	m
Max. z_0	0.306	0.400	0.500	m
$\langle z_0 \rangle$	0.0021	0.0021	0.0021	m
$\langle z_{0\,land} \rangle$	0.0853	0.0841	0.0842	m
Fraction land	39	39	39	%

The maps have slightly different size. Still, the average roughness of the different maps are the same (Table 4). Naturally, the extreme values are greater on the grids with higher resolution. The maximum height of the original data set is 1002 m.

The grid of KAMM had 25 levels from the surface to a height of 4000 m. The lowest grid levels were at 15, 43, 84, 138 m a.g.l. for a grid point at sea level.

7.2 Geostrophic wind over Ireland

The large-scale forcing was determined from 34 years of the geopotential height of the 1000, 850, 700, and 500 hPa level and temperature and humidity at 850 and 500 hPa of the NCEP/NCAR-reanalysis for 1965-1998 (Kalnay et al., 1996). The data were inter- and extrapolated to the heights 0, 1450, 3000, and 5500 m, and a geostrophic wind was calculated at these heights.

Representative classes of geostrophic winds and stratification were determined from the reanalysis data set. The geostrophic wind at 0 m was sorted in 16 sectors and up to 8 speed classes per sector. The classes with the lowest speed were further separated in 3 and 2 stability classes based on a Froude number with the temperature difference between 0 m and 1450 m. The frequency of the classes in one sector is approximately the same except for the lowest and highest speed class. These have lower frequencies in order to get a better representation of higher moments of the wind speed distribution. The classification resulted in a total of 151 classes.

Unfortunately, the Irish wind atlas does not cover the total 34 years. Data from many stations is from the period 1989 to 1998. Therefore, the frequency of the classes was determined for this period. Hence, the classification is not optimal, though it still is expected to be good. The geostrophic wind at 0 m and the frequency of the classes is shown in Figure 26 for the point 8.75° W, 53.75° N.

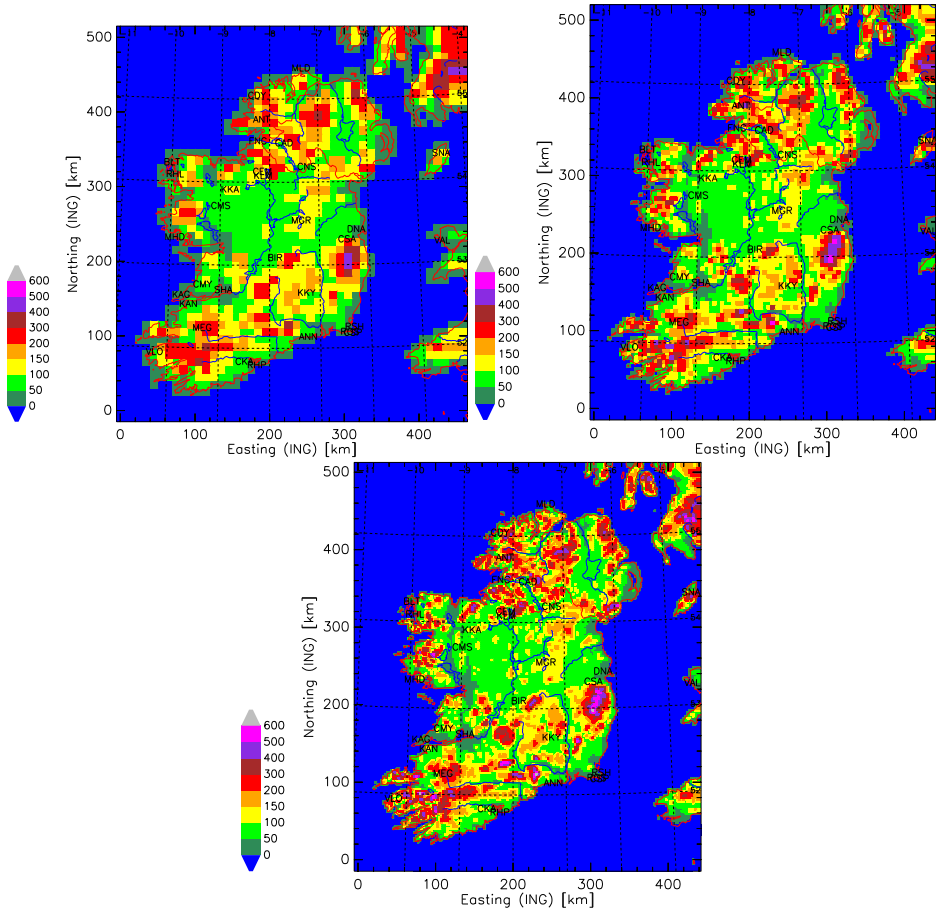

Figure 24. Terrain heights [m] for the 10 km, 5 km, and 2.5 km grid of Ireland. Boundaries and rivers are shown by read and blue lines. The position of observation sites is shown by a code for the station.

The variation of the geostrophic wind across Ireland is shown in Figure 27. The geostrophic wind increases from southeast to northwest.

The geostrophic wind used for the classification and shown in Figure 27 is calculated with a constant Coriolis parameter corresponding to latitude $53.75°$ N because KAMM employs a constant Coriolis parameter. The large-scale forcing for KAMM is an external pressure gradient, which is expressed through a geostrophic wind. Therefore, Figure 27 must show only the variation of this pressure gradient. The variation of the Coriolis parameter is small. Still, it can change the pattern of isolines on such a map.

7.3 Wind resource maps for Ireland

Wind resource maps are again drawn for a height of 50 m a.g.l. of the mean wind speed (Figure 28) and energy flux density (Figure 29). These show the mean of the simulated winds weighted by the frequency of geostrophic wind class.

The main feature is the difference between sea and land. In addition the general decrease of the wind resource from northwest Ireland to southwest Ireland can be recognized. This reflects variation of the large-scale geostrophic wind (Figure 27). The highest values on land occur in the Wicklow Mountains south of Dublin and along the northwest coast.

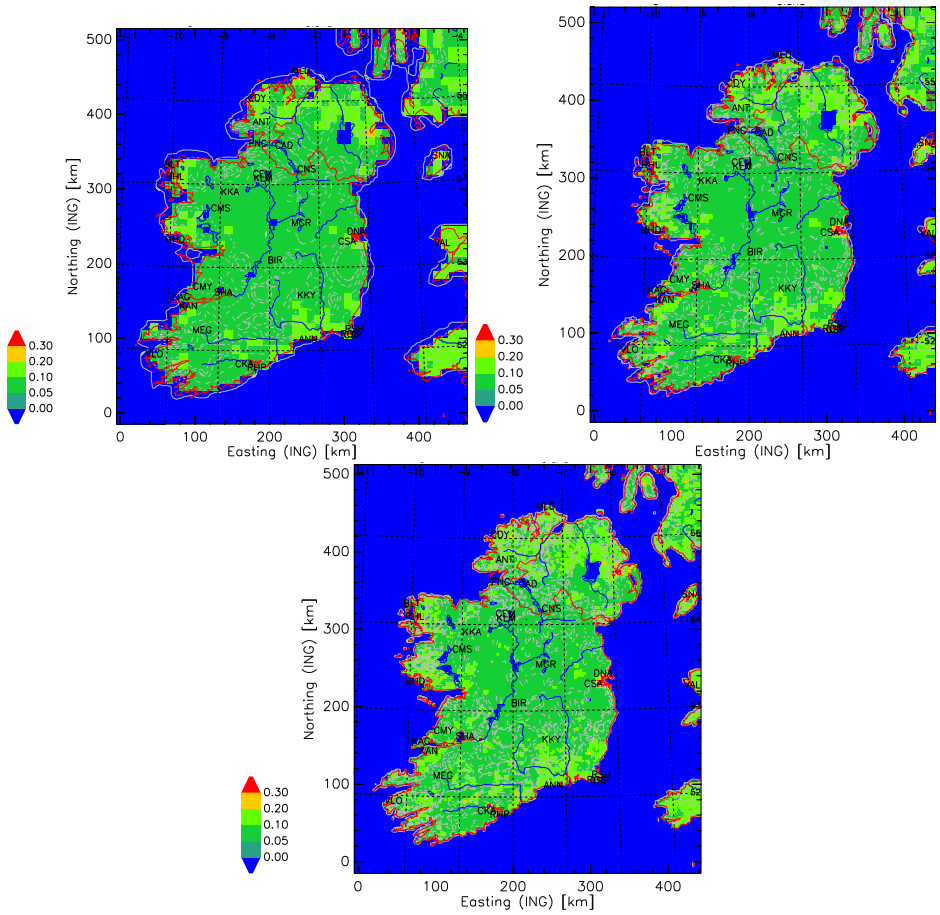

Figure 25. Roughness length [m] for the 10 km, 5 km, and 2.5 km grid of Ireland.

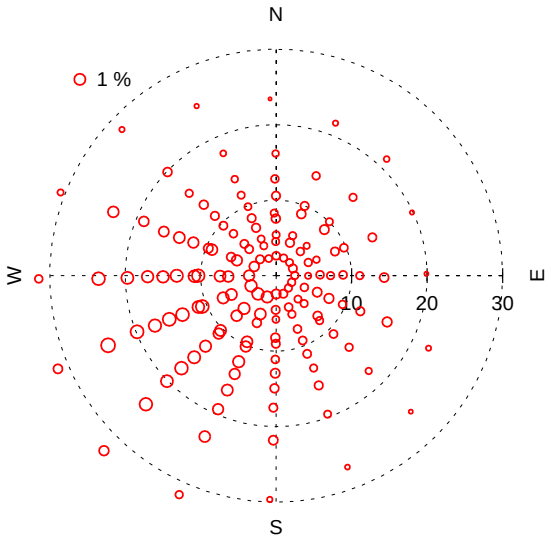

Figure 26. Geostrophic wind at 0 m of the 151 simulation classes for Ireland. The size of the circles is proportional to the frequency at 8.75°W, 53.75°N.

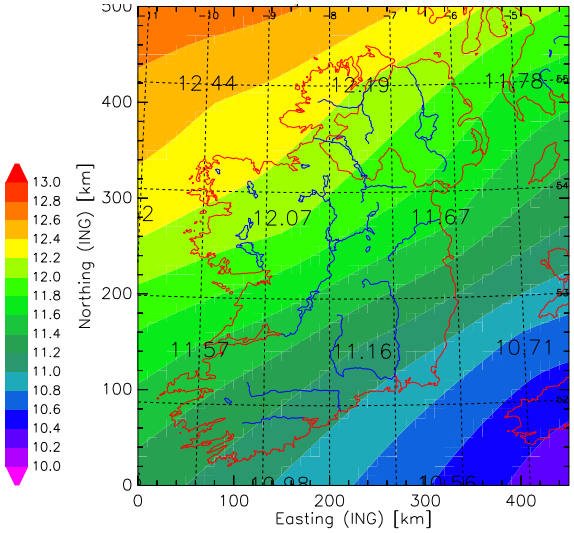

Figure 27. Variation of the geostrophic wind at 0 m over Ireland.

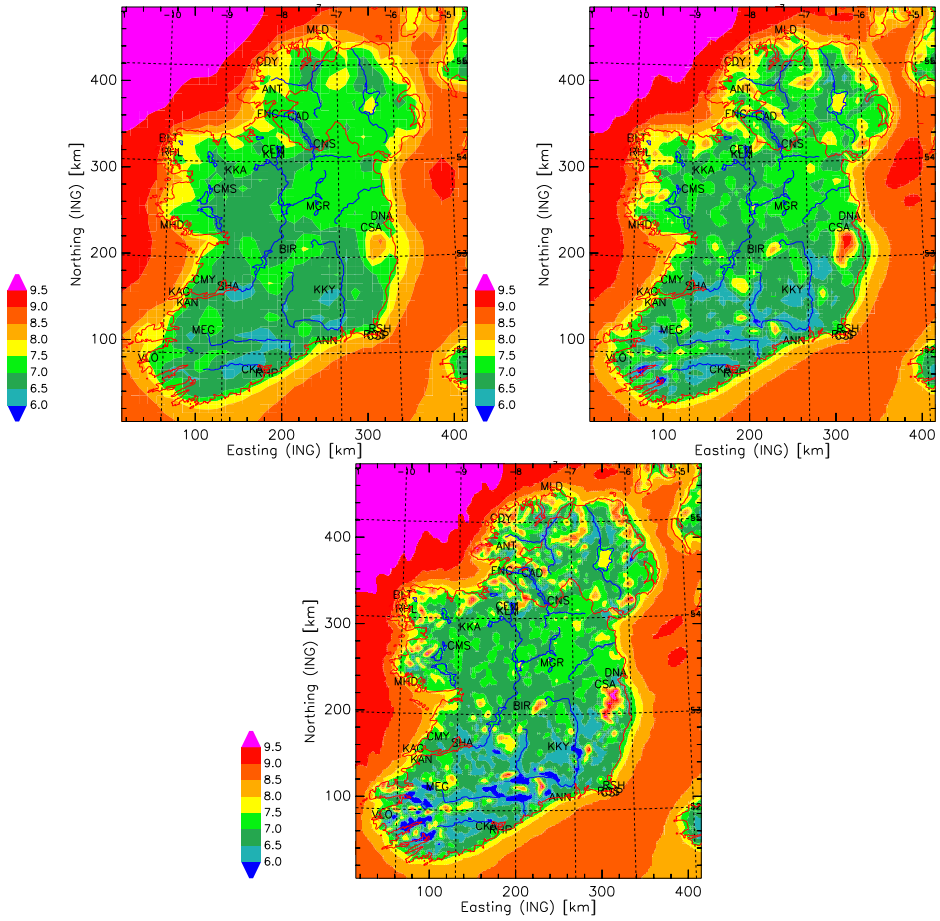

Figure 28. Maps of the mean speed, U $[m\,s^{-1}]$, at 50 m a.g.l. as calculated by KAMM with grid size 10 km (top left), 5 km (top right), and 2.5 km (bottom).

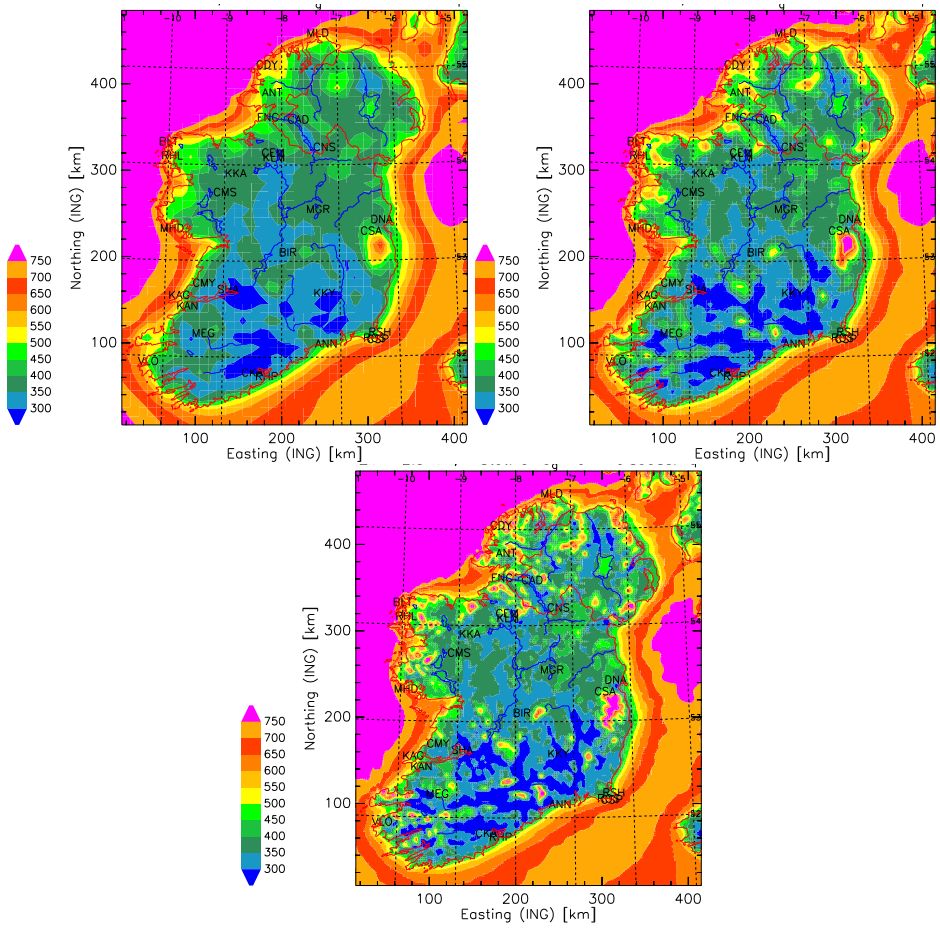

Figure 29. Maps of the energy flux density, E [$W\,m^{-2}$], at 50 m a.g.l. as calculated by KAMM.

7.4 Wind atlas Maps for Ireland

Wind atlas maps were calculated for 50 m a.g.l. above roughness length 3 cm. They are shown in Figures 30 and 31. Again the windiest areas are the Wicklow Mountains and the extreme northwest near the site Clady (CDY).

The contrast between sea and land is reduced. Still, as for Denmark, the coast can be recognized by a minimum over water east of Ireland, and perhaps, increased values on land along the west coast. However, the west coast is also mountainous, and the speed-up of greater mountains is not removed by the orographic correction.

7.5 Comparison with observations

Comparisons are done for stations which will be used in a new Irish Wind Atlas. The analysis of these sites is not complete as the Irish Ordonnance Survey is issuing new maps for Ireland, which shall be used for the new wind atlas. However, big changes are not expected. The station Clones shows much less wind than the other Irish stations. This does not seem correct. It is a station which shall be reanalyzed. It is not included in the comparisons below.

The ruggedness index for most sites is zero. The highest average value is $RIX = 4$ for the station Annestown (ANN). The highest value in an individual sector is 15 which occurs at Annestown and Knocknagarhoon (KAG). At all stations the ruggedness index

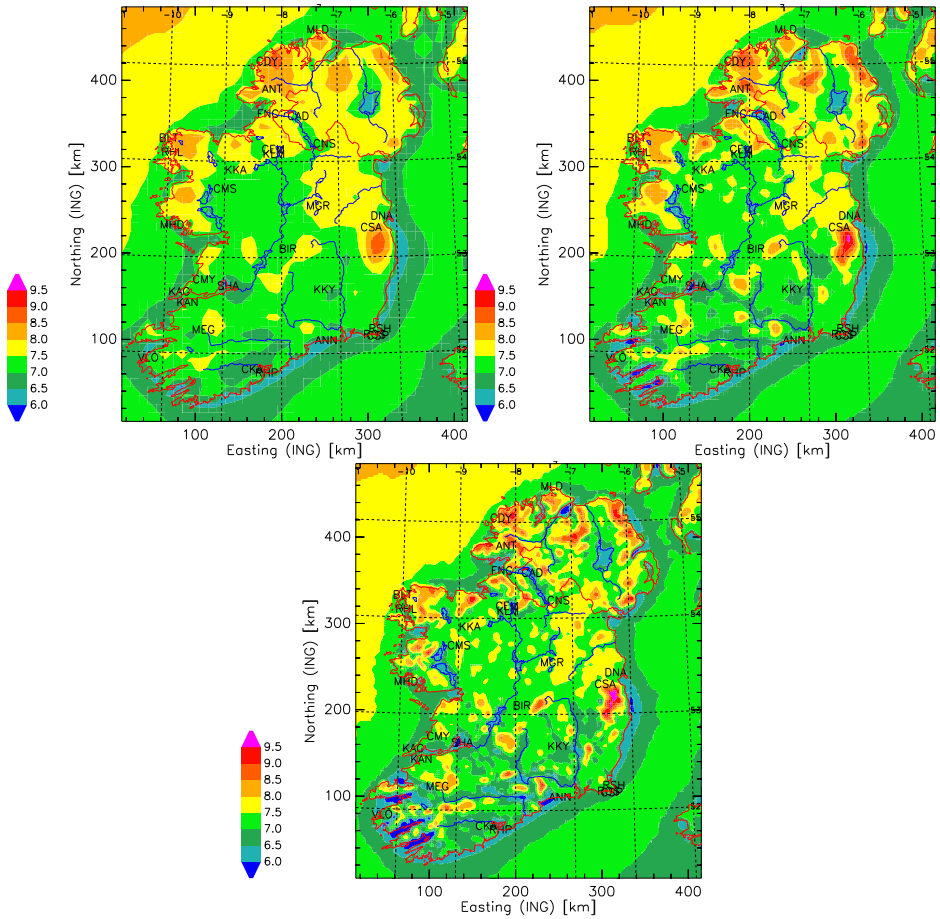

Figure 30. Maps of the mean speed, U $[m\,s^{-1}]$, at 50 m a.g.l. above 3 cm roughness calculated by KAMM.

is zero in most sectors. Therefore, the WASP analysis is very reliable for all stations in Ireland.

Mean wind speed, wind direction, energy flux density, and annual energy production of a Vestas V47 (660kW) turbine at 50 m above 3 cm roughness are compared in Figures 32 and 33. Wind atlas files from the nearest grid point over land are used in the comparison. This is slightly better than comparing atlas files from the nearest grid point.

Again, there is no significant difference between using a 10 km, 5 km, or 2.5 km grid. This shows that the wind atlas concept is valid, and that the corrections applied to the simulations are correct.

Predictions for the exact positions of the observations using only KAMM or using KAMM and WASP can be compared in Figures 34 and 35. The observations heights range from 10 m to 40 m a.g.l.. The simulations with KAMM improve slightly with increasing resolution. But, this improvement is negligible compared to the combination of KAMM and WASP.

It is also possible to make predictions with WASP using only upper-air or geostrophic wind data, i.e. without running a meso-scale model. In order to do this histogram files were made of the wind at 850 hPa from the NCEP/NCAR reanalysis for the years 1989-1998 and every $2.5°$ longitude and latitude, where data was available. Then wind atlas files were generated with WASP. These wind atlas files were interpolated with the LibIntLT-program (Nielsen, 1999) to the exact locations of the Irish stations. Then, the

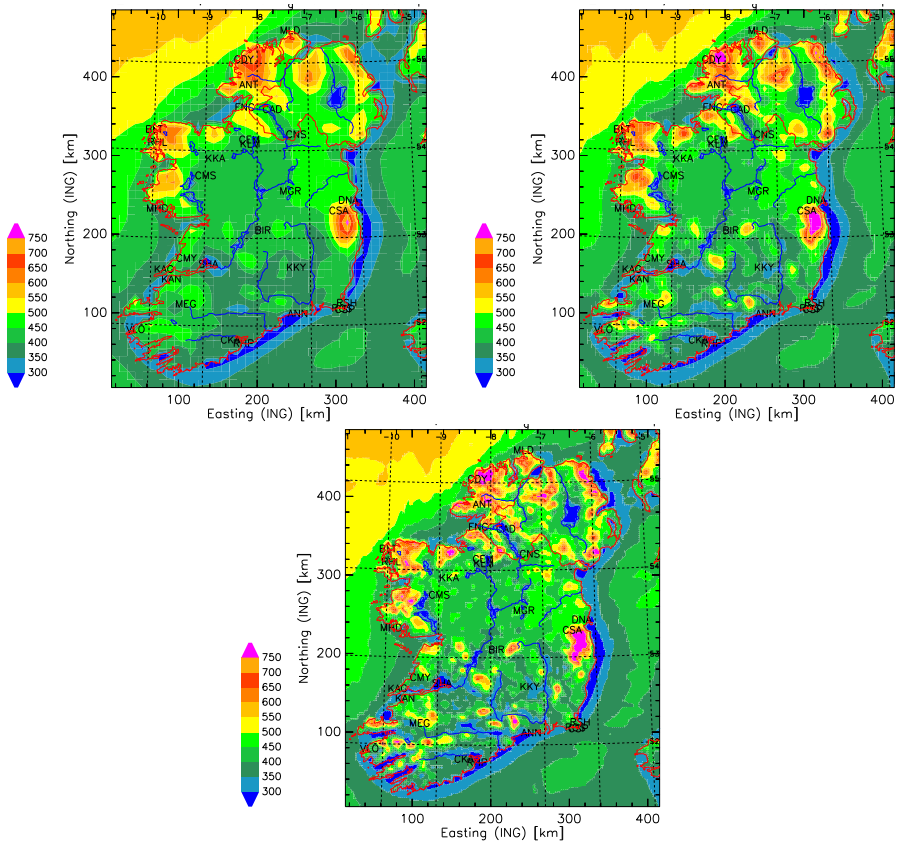

Figure 31. Maps of energy flux density, E [$W\,m^{-2}$], at 50 m a.g.l. above 3 cm roughness calculated by KAMM.

local wind was predicted using this "local" wind atlas files.

The results are shown in Figure 36. The general trend is well captured. The errors are approximately twice as big as using KAMM — with large-scale forcing derived from reanalysis data — and WASP. The relative error of the predicted wind speed decrease with increasing speed because the spread of the predicted Weibull shape parameters, k, is much less than observed. The windy sites have k-parameters greater than two, whereas the shape parameter is closer to 1.5 for the poor sites. The Weibull shape parameter of the upper-air wind does not change much across Ireland. It is close to 1.8 and 1.9 . The local prediction with WASP does not strongly effect the shape of the wind distribution. Therefore, the wind speed prediction tends to become better for the windy sites.

Tests were also made of another way of combining KAMM and WASP. The simulations results were not corrected for roughness changes or orographic speed-up on the meso-scale grid. Instead the predictions, which were made with WASP used only a map with a diameter of the grid size, i.e. WASP only sees the small-scale topography not resolved by the meso-scale model. This yields predictions which are similar, though slightly inferior, to the other combination of KAMM and WASP were the KAMM results are corrected for topographic variations resolved by the grid.

If KAMM results are not corrected for topographic variations, the predictions become worse with decreasing grid size of KAMM. This can be expected because upstream effects become more important for the simulated surface wind. These effects are not removed in the generation of the wind atlas file. Neither can they be accounted for correctly in the prediction with WASP, because WASP cannot see them with a small map. Therefore,

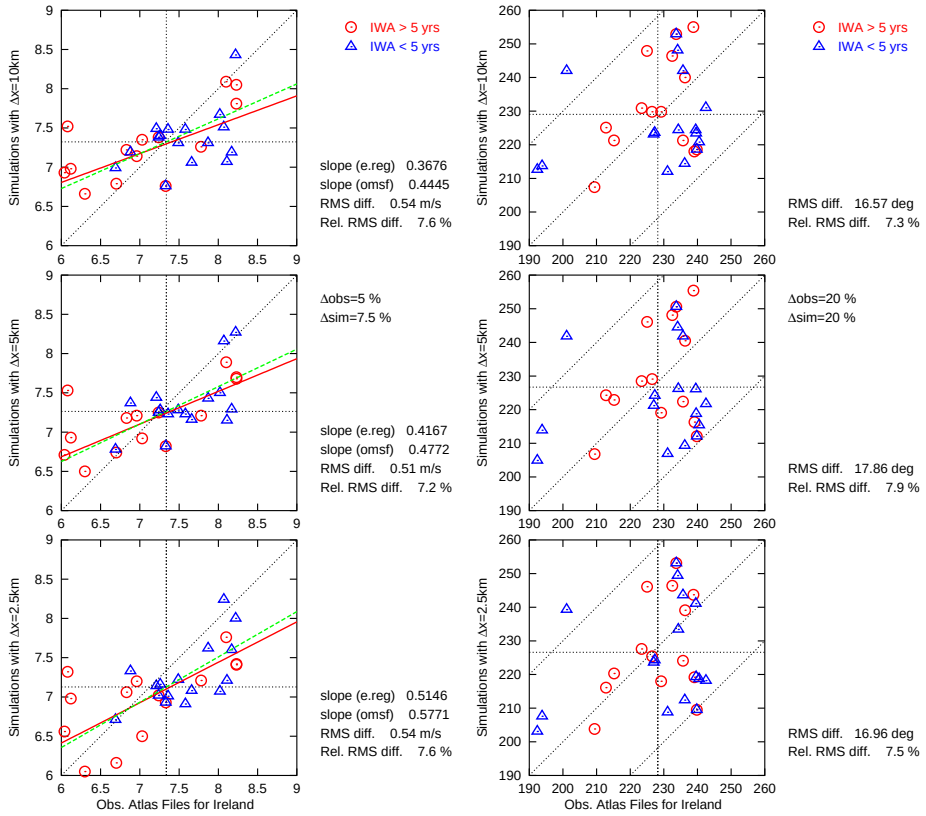

Figure 32. Comparison of wind atlas values derived from observed winds and from simulated winds. Shown are mean speed, U (left), and mean vector wind direction, DD (right), at 50 m a.g.l. above 3 cm roughness.

for grid sizes of 10 km (or perhaps more), this simpler combination of KAMM and WAsP is applicable, though a bit worse than combination with corrected KAMM results. But, it should not be used for higher resolutions.

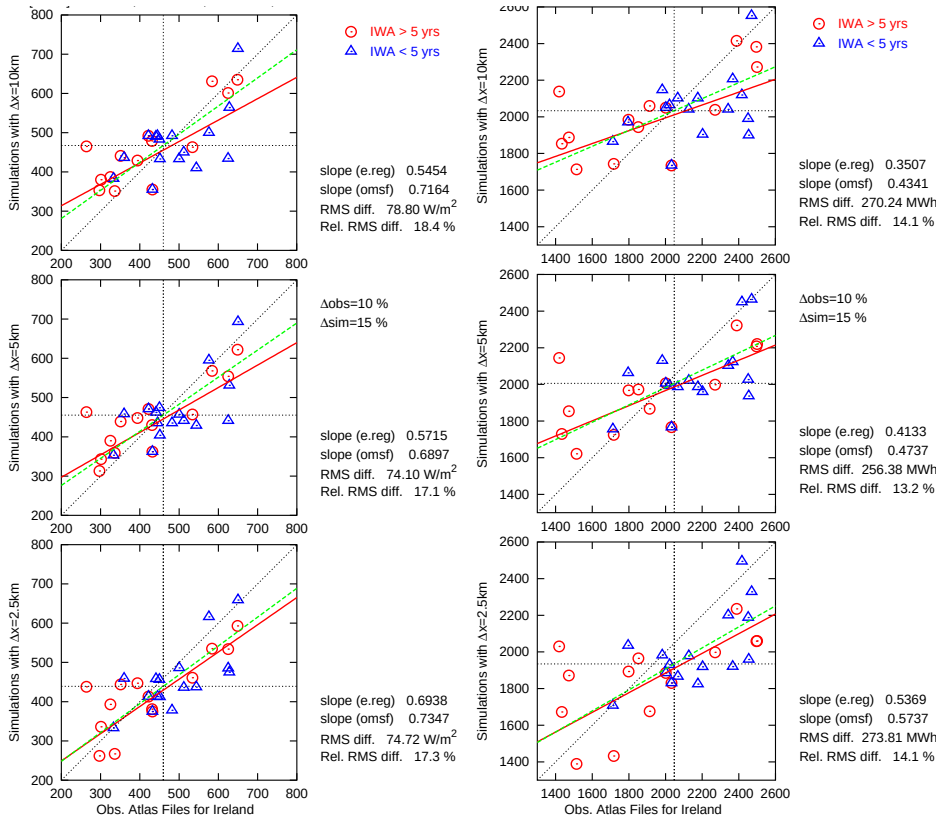

Figure 33. Comparison of wind atlas values derived from observed winds and from simulated winds. Shown energy flux density, E (left), and annual energy production, AEP (right), at 50 m a.g.l. above 3 cm roughness. The power production is calculated for a Vestas V47 (660 kW) turbine, with a hub height of 50 m over a flat site.

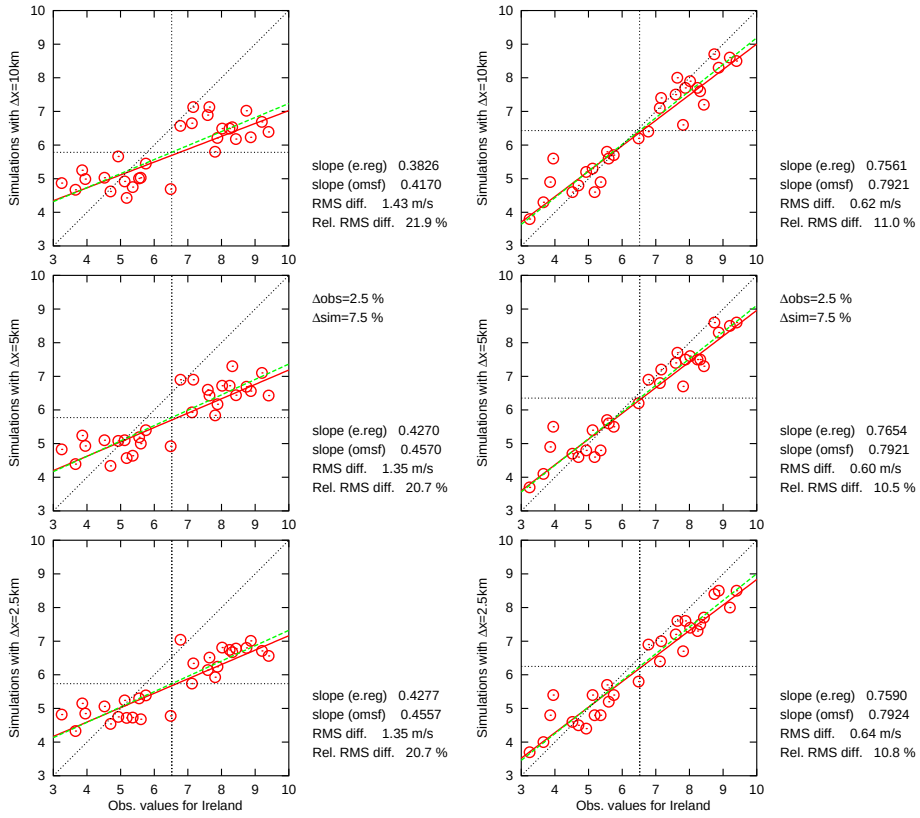

Figure 34. Comparison of the observed wind mean wind speed at sites in Ireland with predictions using only KAMM (left) and predictions using KAMM and WASP (right). The observation heights range from 10 to 40 m a.g.l..

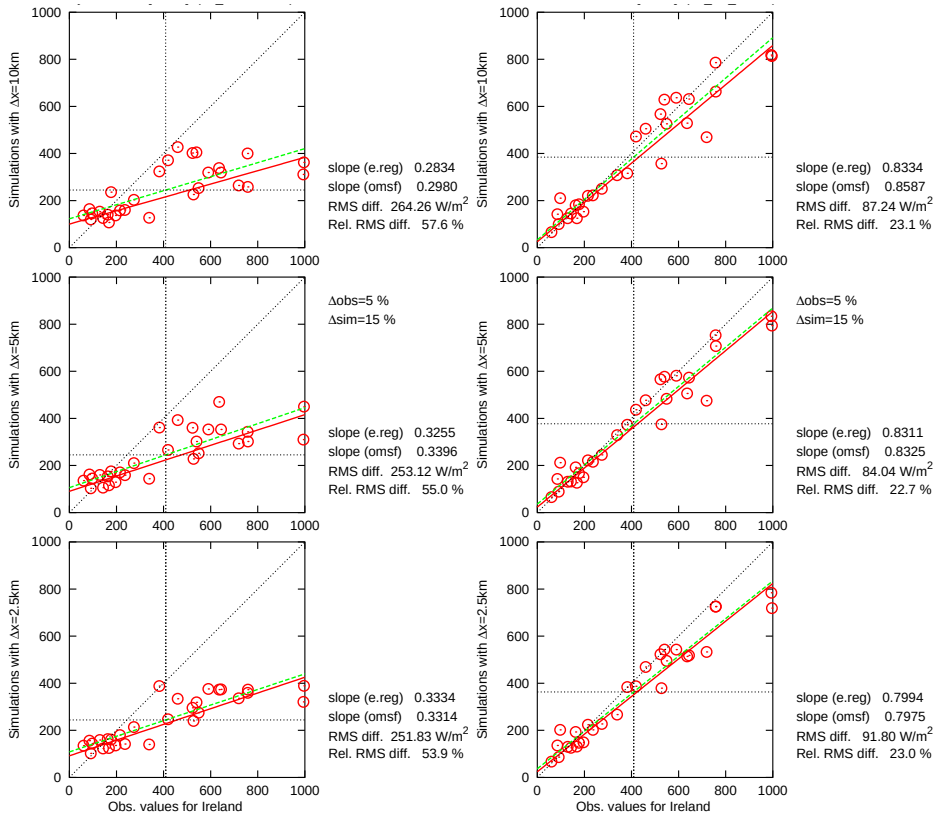

Figure 35. Comparison of the observed energy flux density at sites in Ireland with predictions using only KAMM (left) and predictions using KAMM and WASP (right).

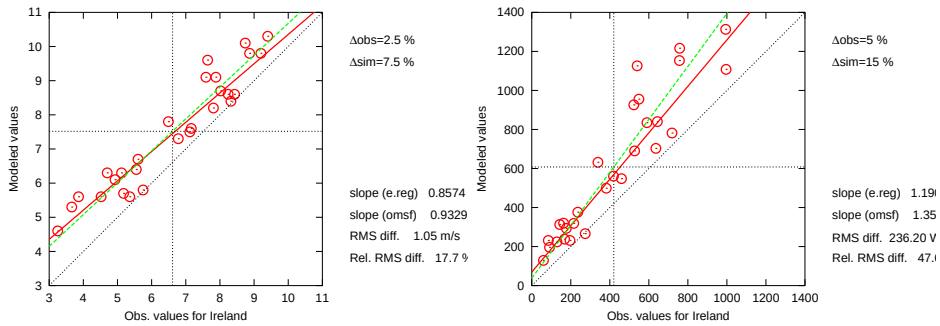

Figure 36. Predictions using only reanalysis data and WASP for stations in Ireland (see text). Prediction for mean wind speed are on the left, and for energy flux density on the right. The abscissa shows the observed values.

8 The Numerical Wind Atlas for Northern Portugal and Galicia

8.1 Topography for Northern Portugal and Galicia

The orography of Northern Portugal and Galicia was derived from the GTOPO30 data base. The land surface roughness was determined from the CORINE data base. In some parts it differed from the GLCC data base. The CORINE data base has higher resolution than the GLCC data base, and we believe it is more accurate. Height maps are shown in Figure 37, and roughness maps in Figure 38. A summary of the topography is given in Table 5.

Table 5. Maximum terrain height, h, and roughness length, z_0, average roughness lengths, $\langle z_0 \rangle$, and fraction of land areas for different maps of Northern Portugal and Galicia.

Δx	10 km	5 km	2.5 km	
Grid size	32×48	60×90	120×180	points
Max. h	1629	1789	1888	m
Max. z_0	0.334	0.423	0.672	m
$\langle z_0 \rangle$	0.144	0.187	0.184	m
$\langle z_{0\,land} \rangle$	0.126	0.125	0.125	m
Fraction land	66	70	70	%

Naturally, the extreme heights are greater on the grids with higher resolution. The 10 km grid map is somewhat greater than the other maps. It includes more sea areas. Therefore, the average roughness length is a bit less. The average roughness of land areas is essentially the same for all maps. (Table 5).

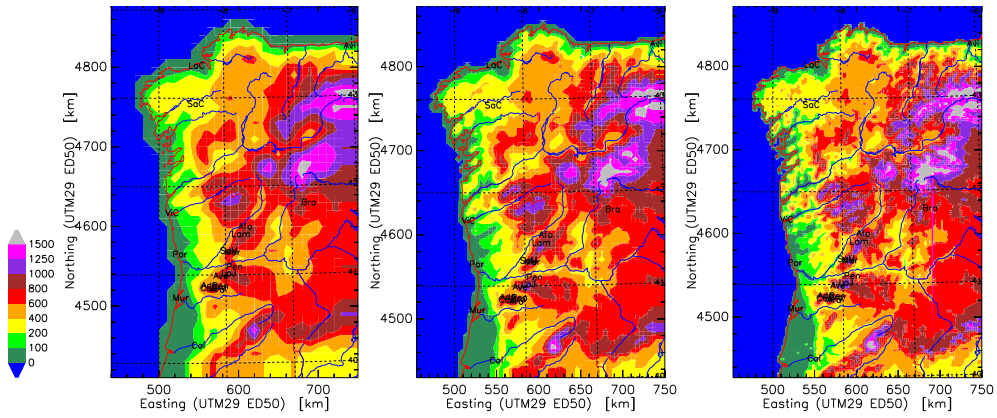

Figure 37. Terrain heights [m] for the 10 km, 5 km, and 2.5 km grid of Northern Portugal and Galicia. Boundaries and rivers are shown by read and blue lines. The position of observation sites is shown by a code for the station.

The size of the horizontal domain is given in Table 5. In the vertical 27 terrain following levels are employed up to 5500 m a.s.l. . For grid points at the sea the lowest grid levels are at 17 m, 50 m, and 98 m above ground level. At greater elevations these levels are closer to the surface in order that the top grid level is at constant height. E.g. at 1000 m

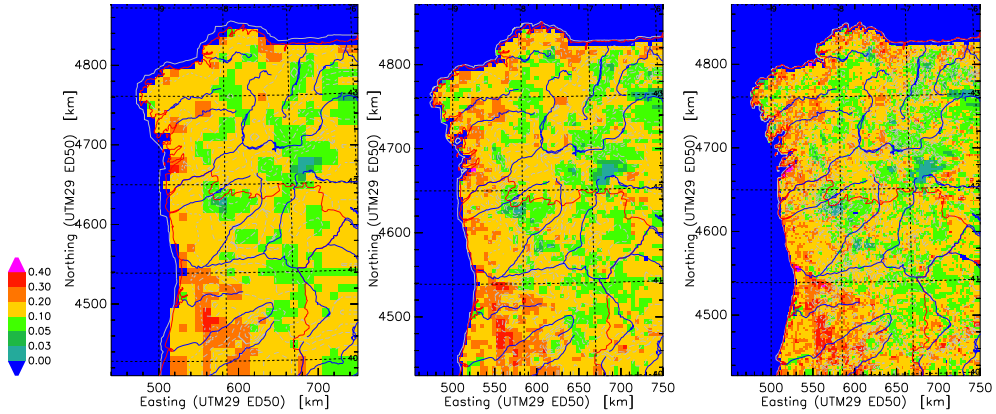

Figure 38. Roughness length [m] for the 10 km, 5 km, and 2.5 km grid of Northern Portugal and Galicia.

above sea level the lowest grid levels are at 14 m, 41 m, and 80 m above ground level.

8.2 Large-scale forcing for Northern Portugal and Galicia

The simulations will be compared with data from the from the European Wind Atlas (Troen and Petersen, 1989), which was measured in the 1970s, and data measured in the 1990s. Therefore, the large-scale forcing was determined from a long period of 34 years from 1965 to 1998. The geopotential height of the 1000, 850, 700, and 500 hPa level and temperature and humidity at 850 and 500 hPa of the NCEP/NCAR-reanalysis for 1965-1998 (Kalnay et al., 1996) were inter- and extrapolated to the heights 0, 1500, 3100, and 5700 m. Geostrophic winds were calculated at these heights.

The geostrophic wind changes significantly within the lowest 1500 m of the atmosphere. This is a quite different situation than for Denmark or Ireland. Figure 40 picks out the wind roses of the geostrophic wind at 1500 m above sea level and at sea level at $8.75°$ W, $41.25°$ N at the center of the simulation domain. The mean speed and third moment of geostrophic wind are roughly equal. However, the directional distribution differs significantly. At sea level, north-easterlies are much more frequent than at 1500 m. The upper-level is well within the west wind zone. But, often, the surface is near the right edge of the high pressure system near the Azores.

The representative classes of the geostrophic wind were determined by the geostrophic wind at 1500 m because the good wind power sites in Northern Portugal are on the mountains near 1000 m altitude. Again 16 sectors with up to 8 speed classes and up to 3 stratification classes were chosen. In total there were 148 classes. A map of the large-scale geostrophic wind is shown in Figure 39.

The model was run with stationary forcing, i.e. without radiation. The soil and sea surface temperature were given by the difference to the initial air temperature at the surface. Separate values are used for sea and land. The differences were obtained from the difference of the 2 m and skin temperature of the reanalysis data. The air temperature will change slightly owing to advection. However, the soil temperature is constant in time. It is not homogeneous, because the initial air temperature decreases with height.

The simulation time of the classes ranged from 3 hours to 7 hours. Classes with weaker geostrophic wind are run longer. The total simulation for all 3 grids time was 691 hours, which is 28.8 days, on the Fujitsu VX1 super computer of the Danish Supercomputing

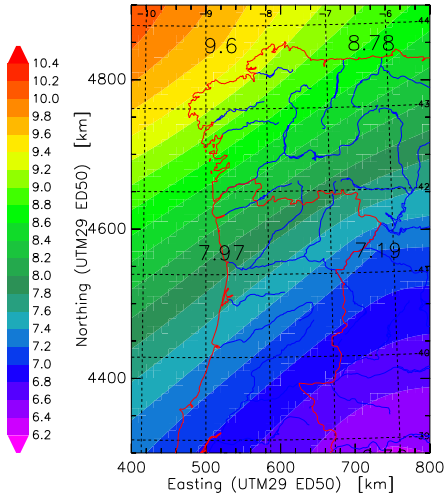

Figure 39. Variation of the geostrophic wind at 1500 m over Northern Portugal and Galicia.

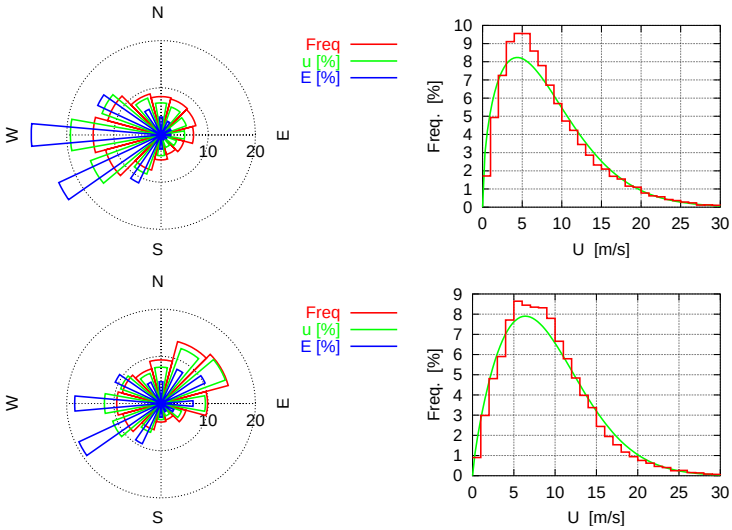

Figure 40. Wind roses of the geostrophic wind at 1500 m (top) and sea level (bottom) at $8.75°$ *W,* $41.25°$ *N at the Portuguese coast from the NCEP/NCAR reanalysis for the years 1965-1998.*

Centre UNI-C and the IBM SP2 computer of Risø.

8.3 Wind resource maps for Northern Portugal

Wind resource maps are again drawn for a height of 50 m a.g.l. of the mean wind speed (Figure 41) and energy flux density (Figure 42). These show the mean of the simulated winds weighted by the frequency of geostrophic wind class.

Over the sea the increase from the south to northwest reflects the variation of the large-scale geostrophic wind (Figure 39). The low-lands of Portugal have relatively low wind resources. However, the area is mountainous and favorable wind power areas occur along mountain ridges. In reality the mountain ridges will have even higher wind resources as the orographic speed-up is greater than modeled with a grid of a resolution of several kilometers.

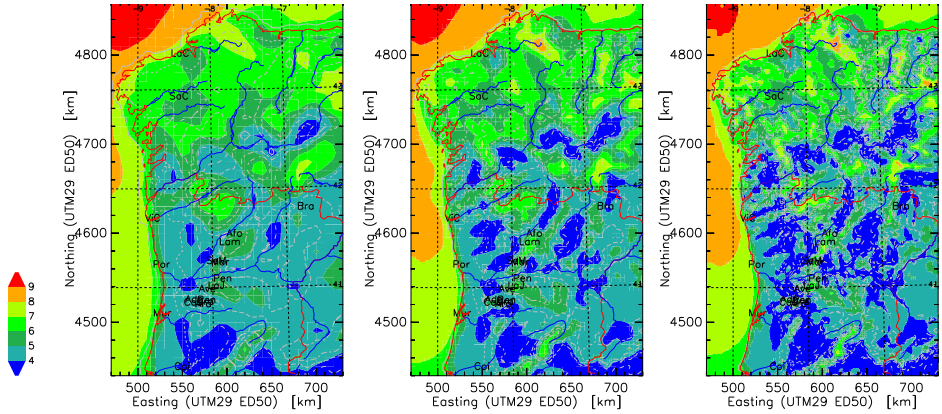

Figure 41. Maps of the mean speed, U [m s^{-1}], at 50 m a.g.l. as calculated by KAMM.

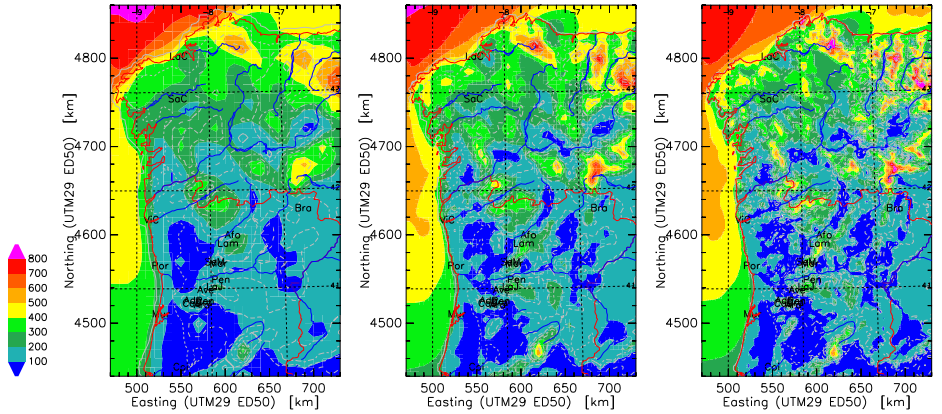

Figure 42. Maps of the mean energy flux density, E [W m^{-2}], at 50 m a.g.l. as calculated by KAMM.

Galicia has generally higher wind resources as the wind increases towards the north on the large scale.

8.4 Wind atlas Maps for Northern Portugal and Galicia

Wind atlas maps of the mean wind speed and mean energy flux density at 50 m above a flat surface with roughness 3 cm are shown in Figures 43 and 44. The major roughness change along the coast is smeared out. It is not easily possible to recognize the coast line.

Most mountain ranges are still clearly visible. This is no deficiency as long as these are meso-scale effects. It can indicate that the orographic corrections applied to the data are too small. Also, it was pointed out that these maps were generated slightly differently than wind atlas files for each grid point. The wind atlas files might be more homogeneous.

The large-scale trend shows increasing wind resource towards the north west as prescribed by the geostrophic winds.

8.5 Comparison with observations

The results from the simulations are compared mainly with 13 stations in Northern Portugal, where the histograms of measured wind and detailed maps are available. Unfortunately, some of this data contain less than 2 years of observations. Hence, the uncertainty

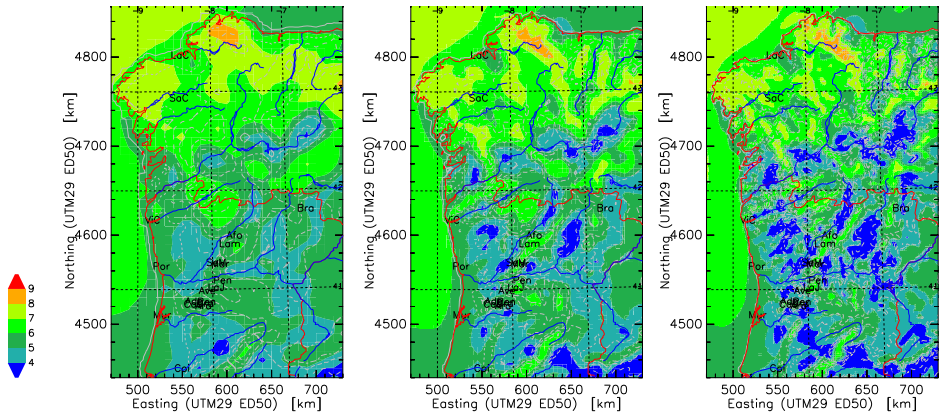

Figure 43. Maps of the mean speed, U [m s^{-1}], at 50 m a.g.l. above 3 cm roughness for Northern Portugal and Galicia.

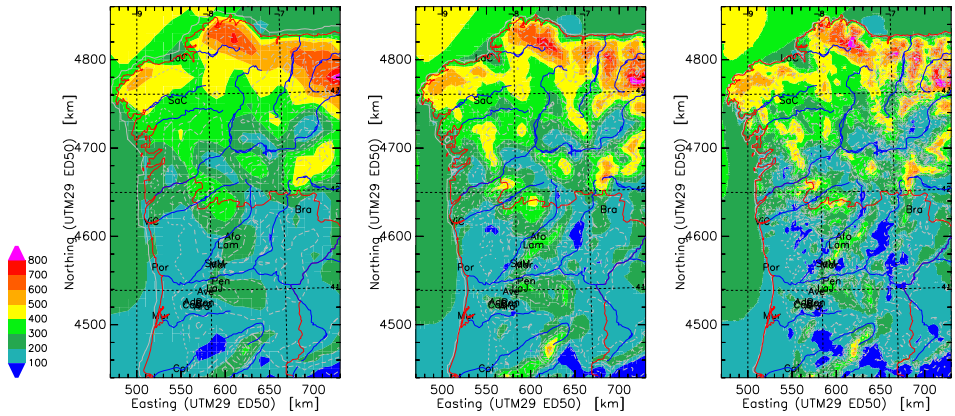

Figure 44. Maps of the mean energy flux density, E [W m^{-2}], at 50 m a.g.l. above 3 cm roughness for Northern Portugal and Galicia.

on the observed mean values can be quite big. Also, the different observation periods will introduce additional differences between simulations and measurements.

Comparing simulation results with observations it appeared that the orographic corrections applied to the simulations tended to be too small. The differences between simulations and observations increased with decreasing grid size of KAMM.

WASP overestimates the orographic speed-up at many of the sites because the terrain is steep and the ruggedness index is much greater than one (Table 2). Therefore, the corrections in WASP are too big, and the mean speed, or energy flux density in the wind atlas data are too small (Mortensen et al., 2000; Bowen and Mortensen, 1996; Mortensen and Petersen, 1998).

In order to combine KAMM and WASP similar corrections must be applied to the simulations. Hence, the program to calculate the orographic flow perturbations was modified, though its smaller values might be more correct. The changes are only small for 50 m a.g.l. or greater heights. The modifications become greater with decreasing height. Only the wind atlas files compared in this section were calculated with the modified version (due to lack of time). For Denmark and Ireland the changes of the results would be very small because the orographic corrections are only small.

The mean wind speed, U, and direction of the mean vector wind, DD, from the wind atlas file at 50 m above roughness length 3 cm are compared in Figure 45. The simulations

on the 2.5 km grid yield the best results: a slope close to one and the smallest RMS-difference and relative RMS-difference. However, there seems to be a systematic bias towards over-prediction.

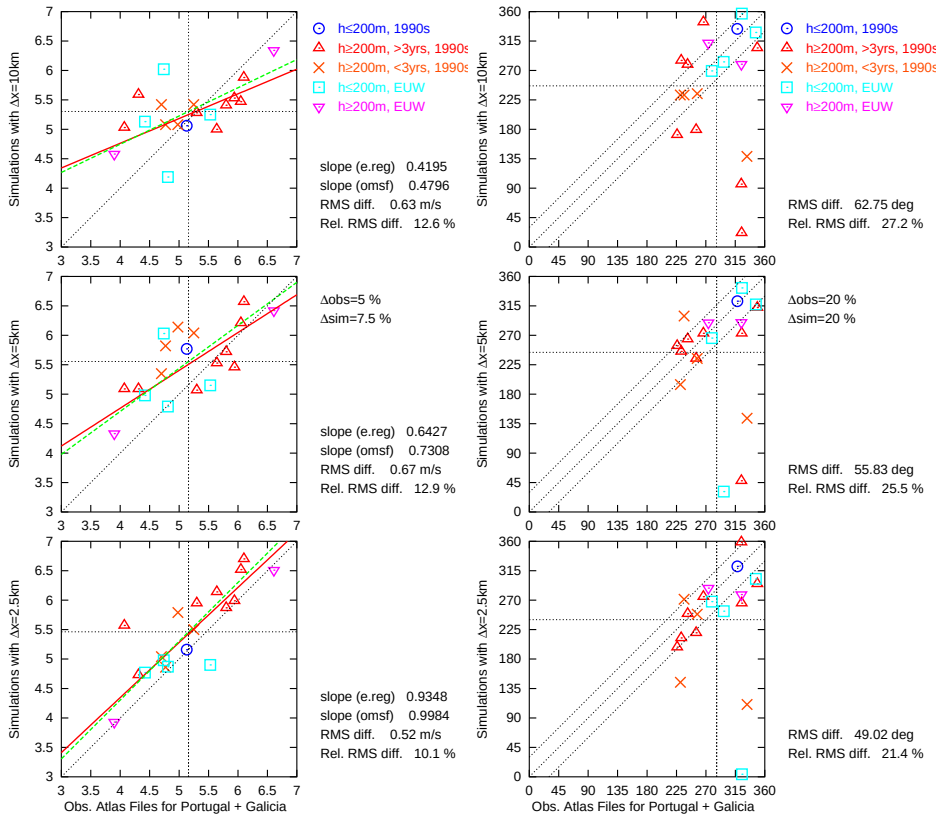

Figure 45. Comparison of wind atlas values derived from observed winds and from simulated winds for Northern Portugal and Galicia. Shown are mean speed, U (left), and direction of the mean vector wind, DD, (right), at 50 m a.g.l. above 3 cm roughness.

Energy flux density, E, and annual energy production, AEP, of a Vestas V47 turbine are compared with wind atlas data from observations in Figure 46. The RMS values of E increase somewhat with decreasing grid size. The AEP has no trend with decreasing grid size. The RMS values of E and AEP are best for the 10 km grid. However, the slopes of the regression line, i.e. the correlation between observation and prediction, is clearly better the smaller the grid size.

Probably, the correlation improves because the altitude of the nearest grid point of the simulation is closer to the true altitude of the station for the smaller grid sizes. This can be important because the distribution of the geostrophic wind varies with height (see Figure 40).

The differences between simulated and observed wind atlas data are bigger than for Denmark or Ireland. However, in this complex terrain modeling errors will be bigger than in smooth terrain with any model. In addition, the uncertainties of the measured data stemming from the short and/or different observations errors are bigger than in Denmark or Ireland.

Predictions for the exact positions of the observations using only KAMM or using KAMM and WASP can be compared in Figures 47 and 48. The observation heights range from 10 m to 30 m a.g.l.. The simulations with KAMM improve with increasing resolution. But, even on the 2.5 km grid the actual values are under-predicted by far. Again the

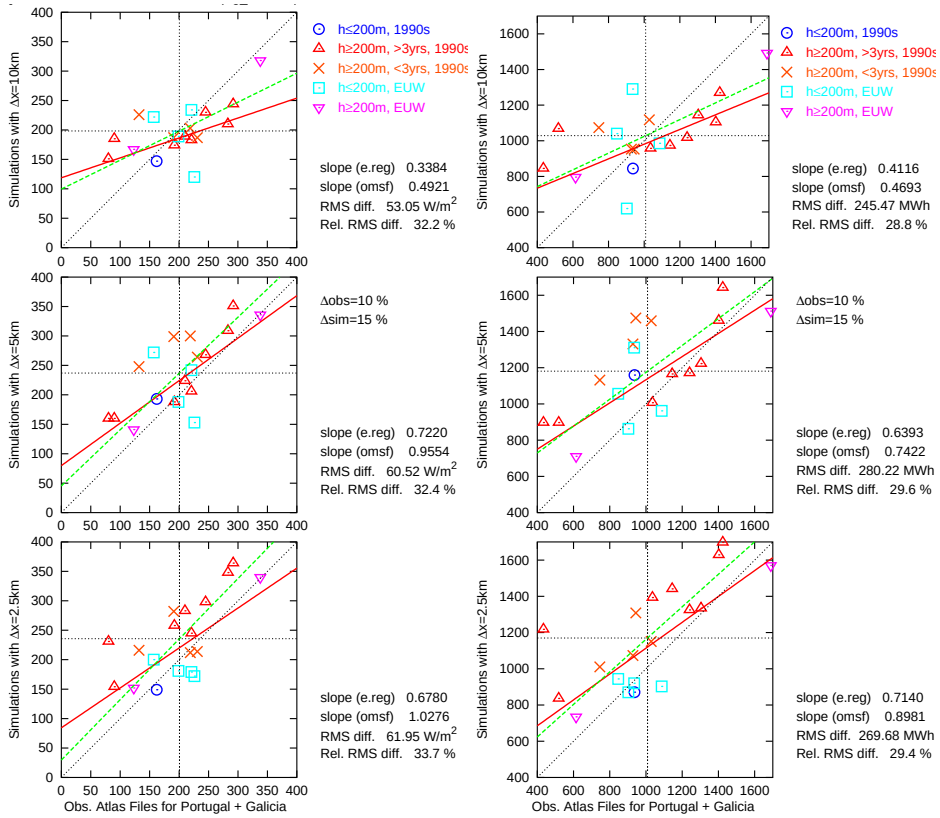

Figure 46. Comparison of wind atlas values derived from observed winds and from simulated winds for Northern Portugal and Galicia. Shown are mean energy flux density, E (left), and annual energy production of a Vestas V47 turbine (right), at 50 m a.g.l. above 3 cm roughness.

combination of KAMM and WASP is much better because the high orographic speed-ups cannot be simulated with a grid size of several kilometers.

The two sites with the highest energy flux density are over-predicted. There are several reasons for this. First, they are the most rugged sites: Senhora de Moreira with $RIX = 30$, and the windiest site Marao with $RIX = 28$. This means that errors of the WASP-predictions must be expected. Second, at both sites the measurements cover less than one year; at Marao less than half a year. Hence, the observed means could deviate strongly from the long-term means. Third, the simulations tend to predict a wind rose which is too narrow. Both sites are located on north-south oriented ridges. The simulations with the 5 km and 2.5 km grid predict – probably – too much strong, westerly wind (Figure 49). Because of the orientation of the ridge winds from this sector are accelerated most. Therefore, the prediction from KAMM and WASP is to high.

The observed wind rose for Marao (Figure 49 top left) may deviate strongly from a climatological wind rose. It contains no observations from February to June.

If the three stations with less than two years of observation are excluded, i.e. Marao, Senhora de Moreira, and Penude ($RIX = 10$) the RMS difference of energy flux density, E, decreases from 181 W m^{-2} to 71 W m^{-2}, the relative RMS difference from 28 % to 25 %, and the slope of the regression line decreases from 1.27 to 1.17 . The corresponding values for the mean speed become 0.5 m s^{-1}, 8.2 %, and slope 1.18 . Considering the steep terrain, the comparison of observed and modeled data is good.

As for Ireland site predictions were made using the simulated wind from KAMM with-

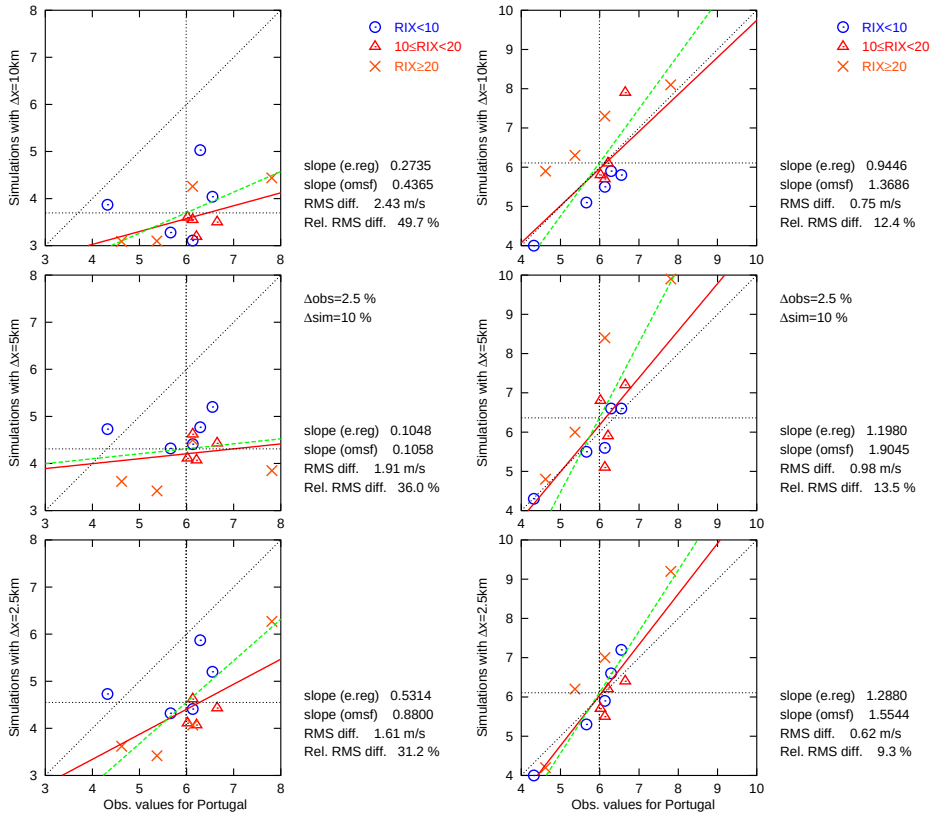

Figure 47. Comparison of the observed wind mean wind speed at sites in Portugal with predictions using only KAMM (left) and predictions using KAMM and WAsP (right). The observation heights range from 10 to 30 m a.g.l..

out corrections and clipped maps corresponding to the grid size of the KAMM with WAsP. It is not as good as correcting the simulations of KAMM when the wind atlas files are generated. For simulations on the 10 km grid the modelling error is only slightly poorer — relative RMS difference of U and E worse by 2 % and 5 %, respectively. However, for the smaller grid sizes the errors increase rapidly with decreasing grid size. This clearly demonstrates that the results of the meso-scale simulations must be corrected for the topographic variations on the model grid before it can be used by WAsP if the model grid size is less than approximately 10 km.

8.6 Simulations with daily radiation cycles

Several tests were made simulating daily cycles of radiation and the developing wind field. The large-scale geostrophic forcing was constant as for the unstationary simulations, but, thermal forcing was added through the diurnal radiation cycle. This is the southernmost area of our simulation regions. Hence, thermal effects should be stronger than at the other regions. Simulations have been made using different initial data. The results were not good.

The geostrophic wind was determined from the NCEP/NCAR reanalysis for the years 1971-1999 because observations were available for this period. However, *no* station data was available for the full period.

The data was divided into four subsets: spring from 16 March to 15 June, summer from 16 June to 15 September, fall from 16 September to 15 December, and winter from 16

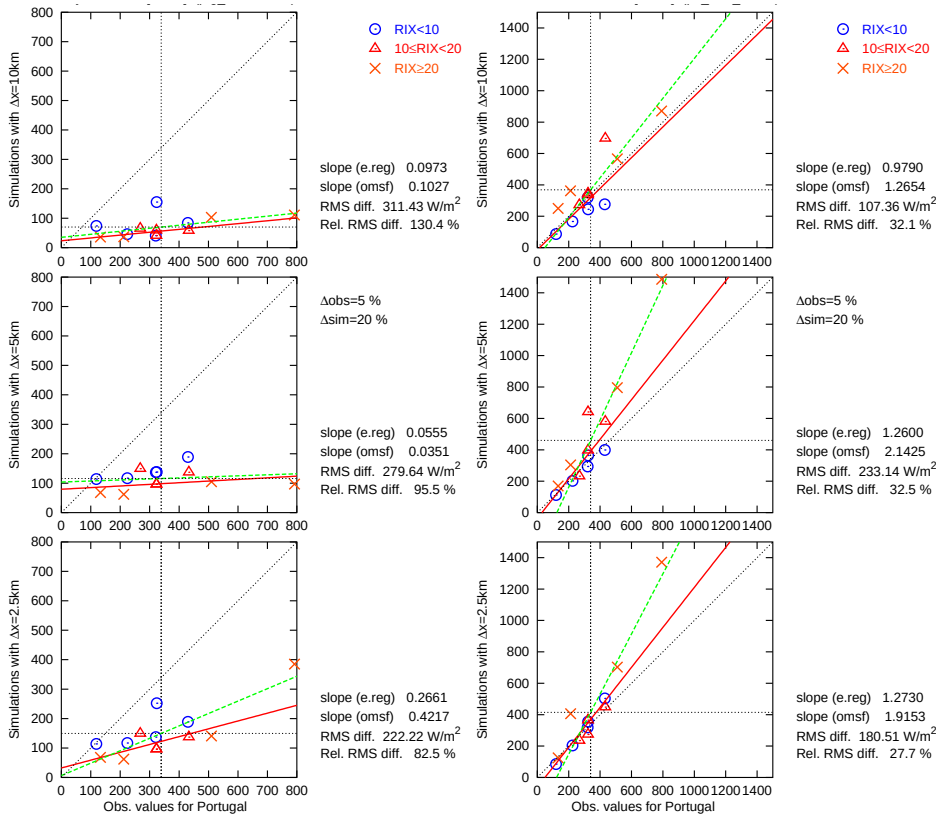

Figure 48. Comparison of the observed energy flux density at sites in Portugal with predictions using only KAMM (left) and predictions using KAMM and WASP (right).

December to 15 March. This division was made expecting different temperature contrasts between sea and land, which might influence the development of sea breezes.

The geostrophic wind data for each season was represented by 12 sectors with up to 5 speed classes yielding a total of 224 classes.

The initial sea and soil surface temperatures were determined from the reanalysis data at 0 UTC. The initial temperature difference between air and soil was set to the mean difference between the 2 m-temperature and the skin or sea surface temperature of the reanalysis data of the geostrophic wind classes. Only the simple soil model of KAMM (Bhumralkar, 1975) was used. With the soil-vegetation model of Schädler (1990) input data for vegetation type, soil type, temperature and humidity in several layers is needed. As this information is not known, educated guesses would have to be made. Therefore, it was assumed that a simpler model might be almost as good as the more complete soil-vegetation model.

The day which was in the middle of the seasons defined above was simulated. The simulations started at 6 UTC. A full daily cycle, i.e. 24 hours, was simulated. However, in many simulations unrealistically high winds developed. Results will not be shown. Probably, the estimates for the initial soil or sea surface temperatures were too rough. Also, the force-restore soil model might be too simple.

A major reason for doing simulations of a full daily cycle was the expectation to get wider wind roses. Especially, the hope to simulate sea breezes or cold air drainage with significant changes in wind direction. This could be realized for some cases with very weak geostrophic winds. For most simulations the variation of the wind direction over the course of the day was only small. Hence, it might be better to use more sectors for the

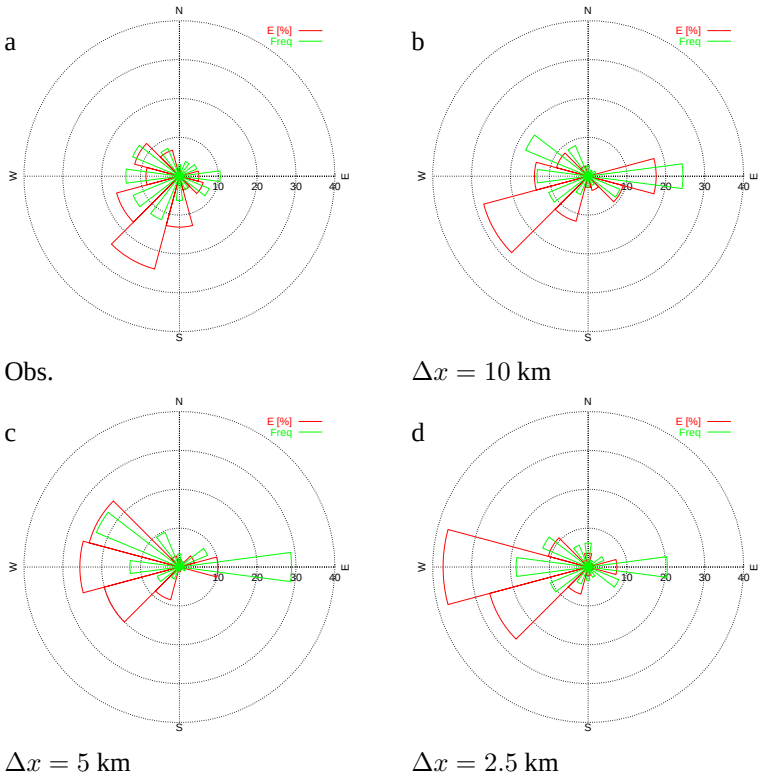

Figure 49. Comparison of the wind rose from the wind atlas data for Marao at 25 m above roughness length 3 cm: a) From observations, b) simulations with $\Delta x = 10$ km, c) 5 km), and (d) 2.5 km. The wide sectors in red show the distribution of the energy flux density, E, and the narrow green sectors the wind direction distribution.

geostrophic wind classes.

Perhaps, a combination of simulations without radiation for higher geostrophic winds and simulations with daily radiation cycle of the situations with weak geostrophic wind would yield the best results; i.e. the mean power comes from the stationary simulations and the wider wind rose through the daily cycles.

9 The Numerical Wind Atlas for the Faroe Islands

9.1 Topography for the Faroe Islands

The Faroe Islands are much smaller than the other regions. The terrain is very steep with many deep, narrow fjords. Therefore, it was not considered sensible to make simulations with a grid size of 10 km. Instead simulations were made with grid sizes of 5 km, 2.5 km, and 1 km.

Height maps were derived from the Digital Terrain Elevation Data, Level 1, of Denmark's Forsvarets Forskningstjeneste, which has a resolution of 6 arc-seconds in latitude and 3 arc-seconds in longitude. The resolution of the GTOPO30 data base of 30 arc-seconds would be barely enough for this highly structured terrain.

Land use classes were not available with similar resolution. However, the vegetation of the Faroe Islands is relatively uniform. Therefore, the roughness map was derived from the GLCC data base. It contained a few pixels indicating forest. As there is essentially no forest on the Faroe Islands the roughness values assigned to forest classes were changed to maximal 20 cm (different than in Table 1).

Table 6. Maximum terrain height, h, and roughness length, z_0, average roughness lengths, $\langle z_0 \rangle$, and fraction of land areas for different maps of the Faroe Islands.

Δx	5 km	2.5 km	1 km	
Grid size	24×30	45×60	108×144	points
Max. h	682	727	853	m
Max. z_0	0.132	0.200	0.200	m
$\langle z_0 \rangle$	0.0032	0.0033	0.0034	m
$\langle z_{0\,land} \rangle$	0.074	0.075	0.074	m
Fraction land	8.1	8.2	9.0	%

A summary of the topographic grid maps is give in Table 6. Height maps are shown in Figure 50, and roughness maps in Figure 51.

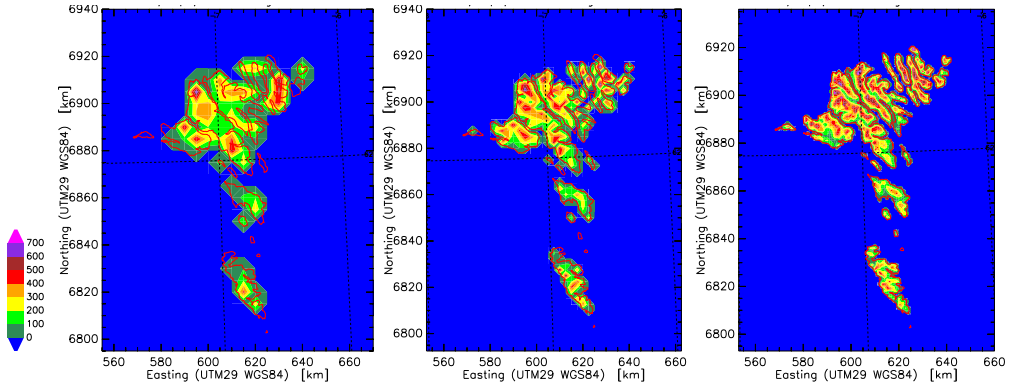

Figure 50. Terrain heights [m] for the 5 km, 2.5 km, and 1 km grid of the Faroe Islands. Coast lines are drawn in red.

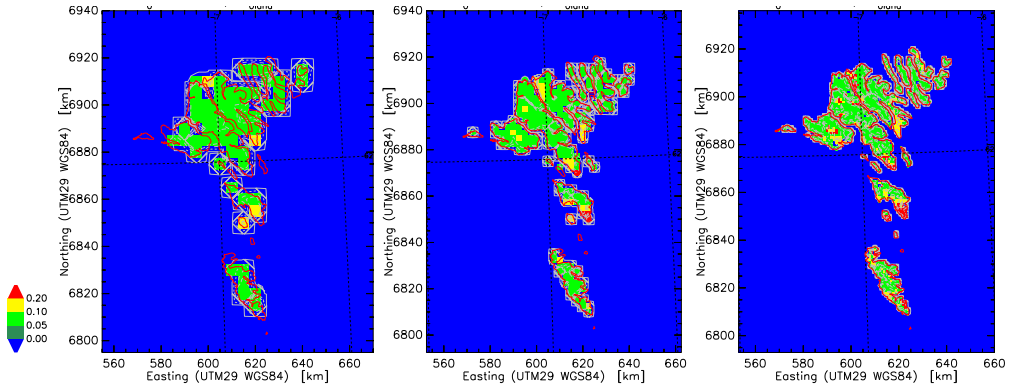

Figure 51. Roughness length [m] for the 5 km, 2.5 km, and 1 km grid of the Faroe Islands.

9.2 Geostrophic wind over the Faroe Islands

The large-scale forcing was determined from 7 years of the geopotential height of the 1000, 850, 700, and 500 hPa level and temperature and humidity at 850 and 500 hPa of the NCEP/NCAR-reanalysis for 1988-1994 (Kalnay et al., 1996). The data was inter- and extrapolated to the heights 0, 1380, 2900, and 5400 m, and a geostrophic wind was calculated at these heights.

Representative classes were determined from the geostrophic wind at 1380 m, It was sorted in 18 sectors and up to 7 speed classes per sector. These are two sectors more than for the other regions. It was thought to be necessary to have a relatively high resolution of direction because the islands have many narrow, deep valleys. Already a small change of the large-scale wind might lead to a big change of the flow in the valley. The classes with the lowest speed were further separated in 1 or 2 stability classes based on a Froude number with the temperature difference between 0 m and 1380 m. The classification resulted in a total of 148 classes.

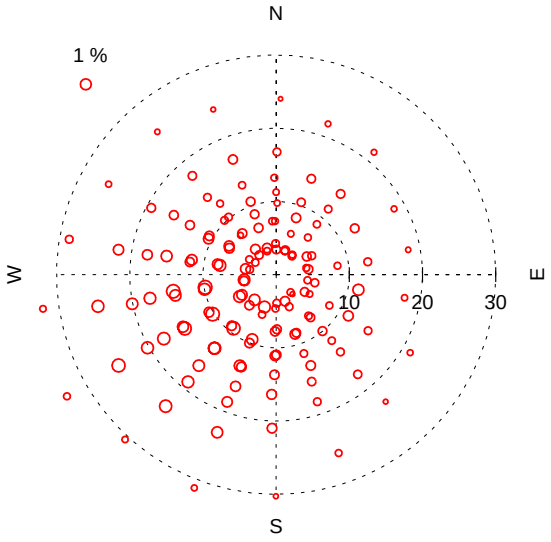

Figure 52. Geostrophic wind at 1380 m of the 148 simulation classes for the Faroe Islands. The size of the circles is proportional to the frequency at 6.25°W, 61.25°N.

The geostrophic wind classes are shown in Figure 52. The most frequent and strongest geostrophic wind comes from Southwest. The strongest geostrophic wind has a magnitude of 33 $\mathrm{m\,s^{-1}}$ from 240°. It has a frequency of 0.391 %, or 1.4 days per year. The

mean strength of the geostrophic wind is 11.4 m s^{-1}.

9.3 Wind resource maps for the Faroe Islands

Wind resource maps are shown for a height of 50 m a.g.l. in Figure 53 for mean wind speed and in Figure 54 for mean energy flux density. As expected the highest wind resource is predicted along the mountain ridges. The fjords are relatively sheltered areas. On the 1 km grid there is almost a factor 10 difference between the lowest energy flux of 181 W m^{-2} to highest value of 1780 W m^{-2}. The mean wind is weaker in the north easter part of the islands which is downwind of the prevailing wind direction.

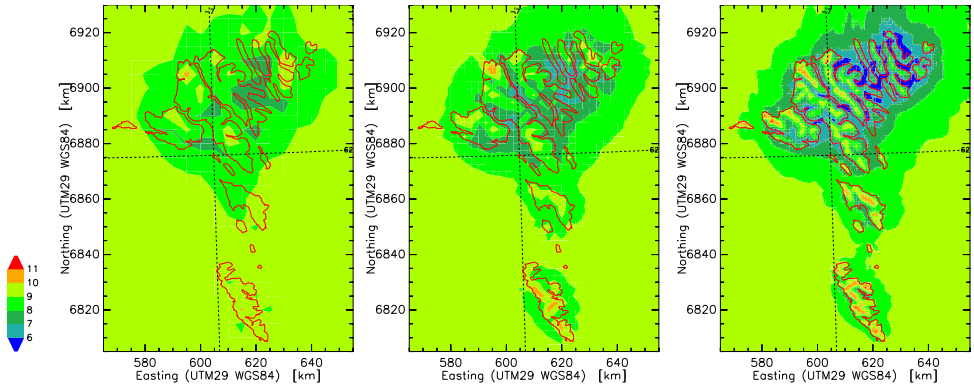

Figure 53. Maps of the mean speed, U [m s^{-1}], at 50 m a.g.l. as calculated by KAMM.

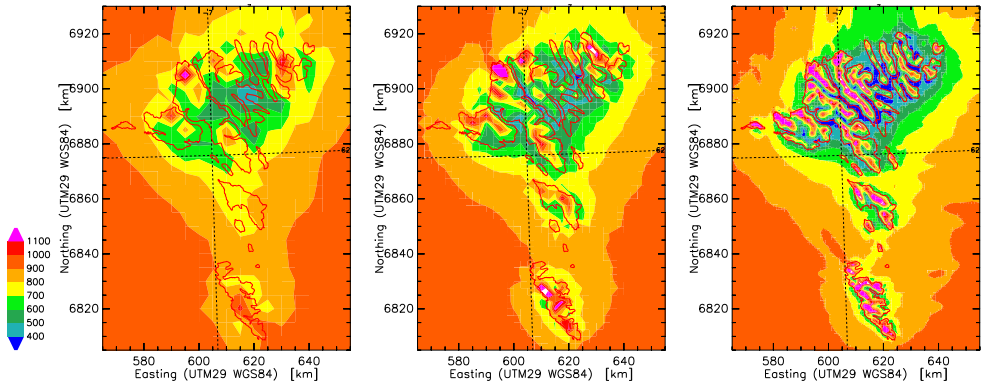

Figure 54. Maps of the energy flux density, E [W m^{-2}], at 50 m a.g.l. as calculated by KAMM.

As the Faroe Islands are very steep it is interesting to determine the contribution of the vertical velocity component, w, to the total speed or the 3. moment of the wind speed from the calculations on the 1 km grid. The difference can be quite large. The mean horizontal wind speed, $\sqrt{u^2+v^2}$, is up to 5 % less than the full wind speed, $\sqrt{u^2+v^2+w^2}$. For the 3. moment, i.e. the energy flux density, the difference is up to 17 %. These values occur at a grid point where the mean horizontal wind speed is 7.5 m s^{-1}. However, wind turbines would probably not be erected at such sites. The big flow inclination might put high loads on the turbine and the control mechanisms for the turbine might have to be specially adapted to such a site.

9.4 Wind atlas Maps for the Faroe Islands

Wind atlas maps for a height of 50 m above a surface with 3 cm roughness length are shown in Figures 55 and 56. The “wind atlas terrain corrections” are sufficient to remove the sharp gradient between land and sea. However, the variation on land is only weakly reduced. As for the mountains of Northern Portugal this indicates that the orographic correction applied to the simulated winds is too small. This is an item for future model development.

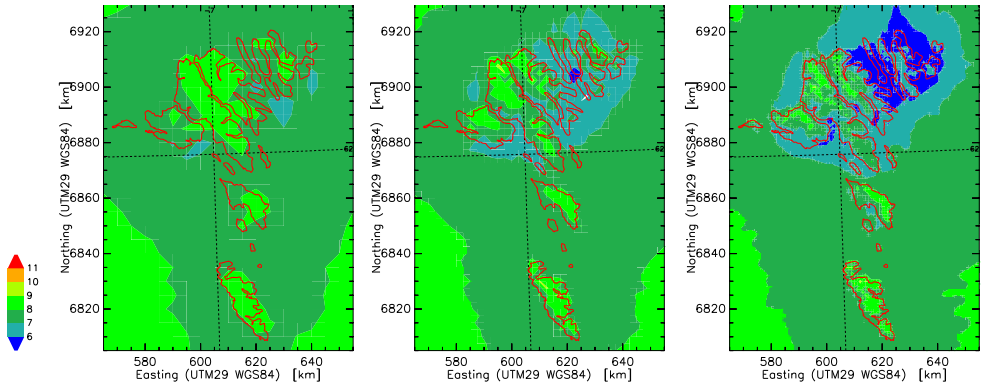

Figure 55. Maps of the mean speed, U [$m\,s^{-1}$], at 50 m a.g.l. above 3 cm roughness for the Faroe Islands.

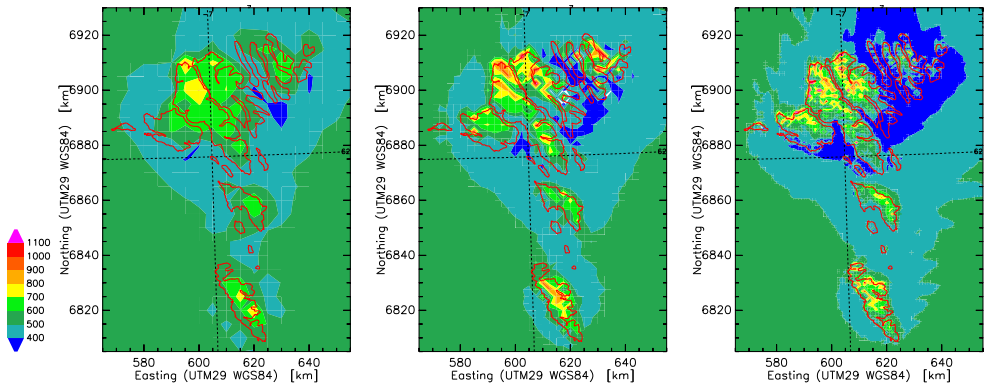

Figure 56. Maps of energy flux density, E [$W\,m^{-2}$], at 50 m a.g.l. above 3 cm roughness for the Faroe Islands.

Unfortunately, no comparison with observations can be made. Preliminary analyses with WASP using maps of lesser accuracy proofed what was known before: The Faroe Islands are not “WASP-country”. The terrain is much too steep for a linear flow model. E.g. corrections of the wind direction which are much bigger than a sector can occur. Therefore, a smoothly varying wind atlas map cannot be generated with linear models or model corrections. Perhaps, a new version of WASP, which is under development right now, will be able to make reasonable wind estimations in such terrain. However, any model will be less than accurate in such terrain than in gentle terrain like Denmark or most parts of Ireland.

10 Conclusions

There are several conclusions to draw. The first relates to WASP analysis of observed data. It is recommended that a topographic map around a site should extend 10 km out from it. If there is a major roughness change like a coast line further away in a frequent wind direction this should be included at even greater distances, perhaps up to 20 km away. In mountainous terrain without major roughness changes somewhat smaller maps might be possible because the orographic flow model of WASP reacts on terrain variations on smaller scale than the roughness change model.

Big maps are critical when a wind atlas for a region shall be made. For predictions close to a measurement site — say one or 2 kilometer away — smaller maps might be used because the errors in the analysis of the predictor site and the predicted site will almost cancel.

The main result of the meso-scale modeling is that wind atlas files obtained from simulations with KAMM do not depend on the resolution of the meso-scale model for relatively flat areas like Denmark or Ireland. This means that the WASP-like corrections applied to the simulated winds can account for the "small-scale" variation of the meso-scale topography. Therefore, it must be recommended to use rather big grid sizes for similar regions, either to save computing resources, or to cover a bigger area with the same amount of computing.

For Northern Portugal higher resolution yielded better results than low resolution. However, it is believed that this is linked to the variation of the geostrophic wind with height, which is observed in this area. If the nearest point of the KAMM grid is at a much lower altitude than the observation site, the climate of the large-scale geostrophic wind near the surface is different from that at the observation point. Hence, greater errors must be expected.

It was also shown that a combination of KAMM and WASP yields much better predictions of observed winds than simple interpolation of the meso-scale simulations to the exact location of the observations. The interpolation of the KAMM results to the observation site was better for the 2.5 km grid than for the 10 km or 5 km grid. For Denmark and Ireland the improvement was only very small. Hence, better results can be expected with even higher resolutions of the meso-scale model. To obtain good results in complex terrain with a lot of small-scale variation, the resolution would have to be 1 km or probably better. Then, the meso-scale simulations cannot cover greater regions, which had been one of the advantages compared to small-scale models like WASP.

Future work will be further improvements of the correction models applied to the meso-scale simulation results. The roughness change model of WASP applied to the grid data of KAMM cannot totally remove roughness change effects at coast lines. Perhaps, the roughness change sub-model of LINCOM (Astrup et al., 1996) will agree better with KAMM. LINCOM is a linear flow model similar to WASP's flow models, but operates on regular cartesian grids, However, LINCOM does not employ an upstream roughness, which depends on wind direction. LINCOM only has a mean roughness, which is the same for all wind directions. This must be tested and compared with the present roughness change correction for the generation of wind atlas files.

The model for the orographic corrections of the meso-scale data needs further tests in mountainous terrain. The results for Portugal were promising.

The simulation with daily cycles of radiation and the flow field were not successful. Perhaps, it would have been better to use the soil-vegetation model of KAMM instead

of its older force-restore soil model. In any case, it will be difficult to find representative cases to simulate. Simply adding more simulations will not help as long as it is not clear what initial conditions to use.

Acknowledgements

This project was financed by the Danish Energy Reseach Program (EFP), contract ENS-1363/98–0020.

Rick Watson provided the observed wind data for Ireland. Most of the data analysis for the Danish sites was done within the EFP project "Vindressourcekort for Danmark", contract 51171/97-0002. Data in Portugal was collected within the JOULE project "Measurements and Modelling in Complex Terrain", contract JOUR-CT90-0067. For one site in Portugal data was provided by Scite-Peristyle, S.A. The orography of the Faroe Islands was derived from the digital terrain elevation data, level 1, with permission of Forsvarets Forskningstjeneste. KAMM is used with kind permission of F. Fiedler, University/Research Center Karlsruhe.

Some calculations were done on the Fujitsu computer of the Danish Computing Center UNI-C. Computing time was provided through the bonus program of the Danish Research Council.

The shaded maps were created using the freeware program plplot.

References

G. Adrian. Zur Dynamik des Windfeldes über orographisch gegliedertem Gelände. *Ber. Deutscher Wetterdienst*, 188:142 pp, 1994.

G. Adrian, N. Dotzek, and H. Frank. Influence of thermally induced wind systems on the wind climate of the Baltic Sea analysed by numerical simulations. In A. Zervos, H. Ehmann, and P. Helm, editors, *Proc. EUWEC'96, Göteborg 1996*, pages 608–610. H. S. Stephens & Associates, 1996.

G. Adrian and F. Fiedler. Simulation of unstationary wind and temperature fields over complex terrain and comparison with observations. *Beitr. Phys. Atmosph.*, 64:27–48, 1991.

P. Astrup, N. O. Jensen, and T. Mikkelsen. Surface roughness model for LINCOM. Report Risø-R-900(EN), Risø National Laboratory, June 1996.

C. M. Bhumralkar. Numerical experiments on the computation of ground surface temperature in an atmospheric general circulation model. *J. Appl. Meteor.*, 14:1246–1258, 1975.

A. K. Blackadar and H. Tennekes. Asymptotic similarity in neutral barotropic planetary boundary layers. *J. Atmos. Sci.*, 25:1015–1020, 1968.

A. J. Bowen and N. G. Mortensen. Exploring the limits of WA^{S}P: The Wind Atlas Analysis and Application Program. In A. Zervos, H. Ehmann, and P. Helm, editors, *Proc. EUWEC'96, Göteborg 1996*, pages 584–587. H. S. Stephens & Associates, 1996.

H. Charnock. Wind stress on a water surface. *Q. J. R. Meteorol. Soc.*, 81:639–640, 1955.

G. A. Degrazia. Zur Anwendung von Ähnlichkeitsverfahren auf die turbulente Diffusion in der konvektiven und stabilen Grenzschicht. Report 12, Wiss. Ber. Inst. Meteor. Klimaf. Univ. Karlsruhe, 1989.

Energi- og Miljødata. *Vindressourcekort for Danmark*. DK-9220 Aalborg Øst, 1999. URL `http://www.emd.dk`.

H. P. Frank and L. Landberg. Modeling the wind climate over Ireland. In A. Zervos, H. Ehmann, and P. Helm, editors, *Proc. EUWEC'96, Göteborg 1996*, pages 631–634. H. S. Stephens & Associates, 1996.

H. P. Frank and L. Landberg. Modelling the wind climate of Ireland. *Boundary-Layer Meteorol.*, 85:359–378, 1997.

H. P. Frank and L. Landberg. Numerical simulation of the Irish wind climate and comparison with wind atlas data. In R. Watson, editor, *Proc. EWEC'97, Dublin 1997*, pages 309–312. Irish Wind Energy Association, 1998. ISBN 0-9533922-0-1.

H. P. Frank, S. E. Larsen, and J. Højstrup. Simulated wind power off-shore using different parameterizations for the sea surface roughness. *Wind Energy*, 3:67–79, 2000.

H. P. Frank and E. L. Petersen. The influence of strong inversions on the wind field at Pyhätunturi Fell. In B. Tammelin, K. Säntti, et al., editors, *BOREAS IV, Wind Energy Production in Cold Climates, 31 March - 2 April 1998, Hetta, Finland*, pages 173–180. Finnish Meteorological Institute, 1998.

F. Frey-Buness, D. Heimann, and R. Sausen. A statistical-dynamical downscaling procedure for global climate simulations. *Theor. Appl. Climatol.*, 50:117–131, 1995.

R. Gibson, P. Kållberg, and S. Uppala. The ECMWF re-analysis (ERA) project. *ECSN Newsletter*, 5:11–21, 1997.

C. P. Hugelmann. Differenzenverfahren zur Behandlung der Advektion. Report 8, Wiss. Ber. Inst. Meteor. Klimaf. Univ. Karlsruhe, 1988.

E. Kalnay, M. Kanamitsu, R. Kistler, W. Collins, D. Deaven, L. Gandin, M. Iredell, S. Saha, G. White, J. Woollen, Y. Zhu, A. Leetmaa, R. Reynolds, M. Chelliah, W. Ebisuzaki, W. Higgins, J. Janowiak, K. C. Mo, C. Ropelewski, J. Wang, R. Jenne, and D. Joseph. The NCEP/NCAR 40-year reanalysis project. *Bull. Amer. Meteor. Soc.*, 77:437–471, 1996.

J. B. Klemp and D. R. Durran. An upper boundary condition permitting internal gravity wave radiation in numerical mesoscale models. *Mon. Wea. Rev.*, 111:430–444, 1983.

L. Kristensen. Orthogonal mean square fitting. Risø/VEA, internal note, December 1999.

L. Landberg and R. Watson. The new Irish Wind Resource Atlas. In *Proc. EWEA'94, Thessaloniki, Greece*, volume I, pages 233–237, 1994.

H.-T. Mengelkamp, H. Kapitza, and U. Pflüger. Statistical-dynamical downscaling of wind climatologies. *J. Wind Eng. Ind. Aerodyn.*, 67&68:449–457, 1997.

N. G. Mortensen, D. N. Heatfield, L. Landberg, O. Rathmann, I. Troen, and E. L. Petersen. *Wind Atlas Analysis and Application Program WASP 7. Version 7.0: Help Facility*. Risø National Laboratory, Roskilde, Jan 2000. CD-ROM ISBN 87-550-2667-2.

N. G. Mortensen, L. Landberg, I. Troen, and E. L. Petersen. *Wind Atlas Analysis and Application Program (WASP) Vol. 2: User's Guide*. Risø National Laboratory, Roskilde, Jan 1993. Risø–I–666(v.2)(EN).

N. G. Mortensen, L. Landberg, I. Troen, and E. L. Petersen. *Wind Atlas Analysis and Application Program (WAsP) Vol. 1: Getting Started*. Risø National Laboratory, Roskilde, 2 edition, 1998. Risø–I–666(v.1)(ed.2)(EN).

N. G. Mortensen, P. Nielsen, L. Landberg, O. Rathmann, and M. N. Nielsen. A detailed and verified wind resource atlas for Denmark. In E. L. Petersen, P. H. Jensen, K. Rave, P. Helm, and H. Ehmann, editors, *Wind Energy for Next Millennium. Proc. European Wind Energy Conference, Nice, France, 1–5 March 1999*, pages 1161–1164, London, 1999. James & James.

N. G. Mortensen and E. L. Petersen. Influence of topographical input data on the accuracy of wind flow modelling in complex terrain. In R. Watson, editor, *Proc. EWEC'97, Dublin 1997*, pages 317–320. Irish Wind Energy Association, 1998. ISBN 0-9533922-0-1.

M. Nielsen. A method for spatial interpolation of wind climatologies. *Wind Energy*, 2: 151–166, 1999.

I. Orlanski. A simple boundary condition for unbounded hyperbolic flows. *J. Comp. Phys.*, 21:251–269, 1976.

G. Schädler. Numerische Simulationen zur Wechselwirkung zwischen Landoberflächen und atmosphärischer Grenzschicht. Report 13, Wiss. Ber. Inst. Meteor. Klimaf. Univ. Karlsruhe, 1990.

G. Schädler, N. Kalthoff, and F. Fiedler. Validation of a model for heat, mass and momentum exchange over vegetated surfaces using LOTREX-10E/HIBE88 data. *Beitr. Phys. Atmosph.*, 63:85–100, 1990.

S. D. Schubert, R. B. Rood, and J. Pfaendtner. An assimilated dataset for earth science applications. *Bull. Amer. Meteor. Soc.*, 74:2331–2342, 1993.

A. M. Sempreviva, S. Larsen, N. G. Mortensen, and I. Troen. Roughness change effects for small and large fetches. *Boundary-Layer Meteorol.*, 50:205–225, 1990.

S. D. Smith. Coefficients for sea surface wind stress, heat flux, and wind profiles as a function of wind speed and temperature. *J. Geophys. Res.*, 93(C12):15467–15472, 1988.

I. Troen and E. L. Petersen. *European Wind Atlas*. Risø National Laboratory for the Commission of the European Communities, Roskilde, Denmark, 1989. ISBN 87-550-1482-8.

USGS EROS Data Center. *Global 30 Arc-Second Elevation Data Set*. Sioux Falls, South Dakota, 2000a. URL `http://edcdaac.usgs.gov/gtopo30/gtopo30.html`.

USGS EROS Data Center. *Global Land Cover Characterization*. Sioux Falls, South Dakota, 2000b. URL `http://edcdaac.usgs.gov/glcc/glcc.html`.

N. Wood. The onset of separation in neutral, turbulent flow over hills. *Boundary-Layer Meteorol.*, 76:137–164, 1995.

Bibliographic Data Sheet **Risø–R–1252(EN)**

Title and author(s)

The Numerical Wind Atlas — the KAMM/WASP Method

Helmut P. Frank, Ole Rathmann, Niels G. Mortensen, Lars Landberg

ISBN	ISSN
87–550–2850–0; 87-550-2909-4 (Internet)	0106–2840

Dept. or group	Date
Wind Energy	June 2001

Groups own reg. number(s)	Project/contract No.
1105028-00	ENS-1363/98–0020

Pages	Tables	Illustrations	References
60	6	56	39

Abstract (Max. 2000 char.)

The method of combining the Karlsruhe Atmospheric Mesoscale Model, KAMM, with the Wind Atlas Analysis and Application Program, WASP, to make local predictions of the wind resource is presented. It combines the advantages of meso-scale modeling — overview over a big region and use of global data bases — with the local prediction capacity of the small-scale model WASP. Results are presented for Denmark, Ireland, Northern Portugal and Galicia, and the Faroe Islands.

Wind atlas files were calculated from wind data simulated with the meso-scale model using model grids with a resolution of 2.5, 5, and 10 km. Using these wind atlas files in WASP the local prediction of the mean wind does not depend on the grid resolution of the meso-scale model. The local predictions combining KAMM and WASP are much better than simple interpolation of the wind simulated by KAMM.

In addition an investigation was made on the dependence of wind atlas data on the size of WASP-maps. It is recommended that a topographic map around a site should extend 10 km out from it. If there is a major roughness change like a coast line further away in a frequent wind direction this should be included at even greater distances, perhaps up to 20 km away.

Descriptors INIS/EDB

RESOURCE ASSESSMENT; WIND; MATHEMATICAL MODELS; MAPS; TOPOGRAPHY; DENMARK; IRELAND; PORTUGAL; FAROE ISLANDS

Available on request from:
Information Service Department, Risø National Laboratory
(Afdelingen for Informationsservice, Forskningscenter Risø)
P.O. Box 49, DK–4000 Roskilde, Denmark
Phone (+45) 46 77 46 77, ext. 4004/4005 · Fax (+45) 46 77 40 13